12-hydroxyheptadecatrienoic acid promotes epidermal wound healing by accelerating keratinocyte migration via the BLT2 receptor

Min Liu,[1,2] Kazuko Saeki,[1,2] Takehiko Matsunobu,[2] Toshiaki Okuno,[1,2] Tomoaki Koga,[1,2] Yukihiko Sugimoto,[3] Chieko Yokoyama,[4] Satoshi Nakamizo,[5] Kenji Kabashima,[5] Shuh Narumiya,[6] Takao Shimizu,[7] and Takehiko Yokomizo[1,2]

[1]Department of Biochemistry, Juntendo University School of Medicine, Tokyo 113-8421, Japan
[2]Department of Medical Biochemistry, Kyushu University, Fukuoka 812-8582, Japan
[3]Department of Pharmaceutical Biochemistry, Kumamoto University, Kumamoto 862-0973, Japan
[4]Department of Metabolism and Atherosclerosis, Osaka University, Osaka 565-0871, Japan
[5]Department of Dermatology and [6]Department of Pharmacology, Kyoto University, Kyoto 606-8501, Japan
[7]Department of Lipid Signaling, National Center for Global Health and Medicine, Tokyo 162-0052, Japan

Leukotriene B_4 (LTB_4) receptor type 2 (BLT2) is a G protein–coupled receptor (GPCR) for 12(*S*)-hydroxyheptadeca-5*Z*,8*E*,10*E*-trienoic acid (12-HHT) and LTB_4. Despite the well-defined proinflammatory roles of BLT1, the in vivo functions of BLT2 remain elusive. As mouse BLT2 is highly expressed in epidermal keratinocytes, we investigated the role of the 12-HHT/BLT2 axis in skin wound healing processes. 12-HHT accumulated in the wound fluid in mice, and BLT2-deficient mice exhibited impaired re-epithelialization and delayed wound closure after skin punching. Aspirin administration reduced 12-HHT production and resulted in delayed wound closure in wild-type mice, which was abrogated in BLT2-deficient mice. In vitro scratch assay using primary keratinocytes and a keratinocyte cell line also showed that the 12-HHT/BLT2 axis accelerated wound closure through the production of tumor necrosis factor α (TNF) and matrix metalloproteinases (MMPs). A synthetic BLT2 agonist accelerated wound closure in cultured cells as well as in C57BL/6J and diabetic mice. These results identify a novel mechanism underlying the action of the 12-HHT/BLT2 axis in epidermal keratinocytes and accordingly suggest the use of BLT2 agonists as therapeutic agents to accelerate wound healing, particularly for intractable wounds, such as diabetic ulcers.

CORRESPONDENCE
K. Saeki:
ksaeki@juntendo.ac.jp
OR
T. Yokomizo:
yokomizo-tky@umin.ac.jp

Abbreviations used: 12-HHT, 12(*S*)-hydroxyheptadeca-5*Z*,8*E*,10*E*-trienoic acid; CBA, cytometric bead array; GPCR, G protein–coupled receptor; HETE, hydroxyeicosatetraenoic acid; LTB_4, leukotriene B_4; MDA, malondialdehyde; MPO, myeloperoxidase; NHEK, normal human epidermal keratinocyte; NSAID, nonsteroidal anti-inflammatory drug; PDGF, platelet-derived growth factor; PG, prostaglandin; RE, responsive element; TP, TxA_2 receptor; TxA_2S, thromboxane A_2 synthase.

Skin wound healing is a complex, multi-step process that encompasses various cells, growth factors, cytokines, and components of the extracellular matrix (Baum and Arpey, 2005). An essential feature of a healed wound is the restoration of an intact epidermal barrier. Re-epithelialization is a key event in wound healing and is mainly achieved by keratinocyte migration, proliferation, and differentiation (Coulombe, 2003). The absence of keratinocyte migration at the wound edge is a critical defect related to the clinical phenotype of chronic nonhealing wounds, such as diabetic ulcers (Brem and Tomic-Canic, 2007). However, the exact manner in which keratinocyte migration is regulated during wound healing also remains largely unknown.

The skin is an organ that displays a highly active metabolism of fatty acids, such as prostaglandins (PGs), HETEs (hydroxyeicosatetraenoic acids), and leukotrienes, etc. (Ziboh et al., 2000). Numerous studies showed that lipid mediators are involved in regulating skin inflammation (Serhan et al., 2008; Kendall and Nicolaou, 2013) related to psoriasis (Mayser et al., 2002), ichthyosis (Yu et al., 2005), and contact dermatitis (Miki et al., 2013). Recently, ATL (aspirin-triggered 15-epi-lipoxin A_4), and resolvin D1 and E1 have been reported to enhance wound healing and epithelial cell regeneration via limiting PMN (polymorphonuclear leukocyte) infiltration and directly stimulating epithelial cells (Norling et al., 2011) in many inflammation-driven diseases, such as cantharidin-induced skin blisters in human (Morris et al., 2009) and TNBS

The Rockefeller University Press $30.00
J. Exp. Med. 2014 Vol. 211 No. 6 1063-1078
www.jem.org/cgi/doi/10.1084/jem.20132063

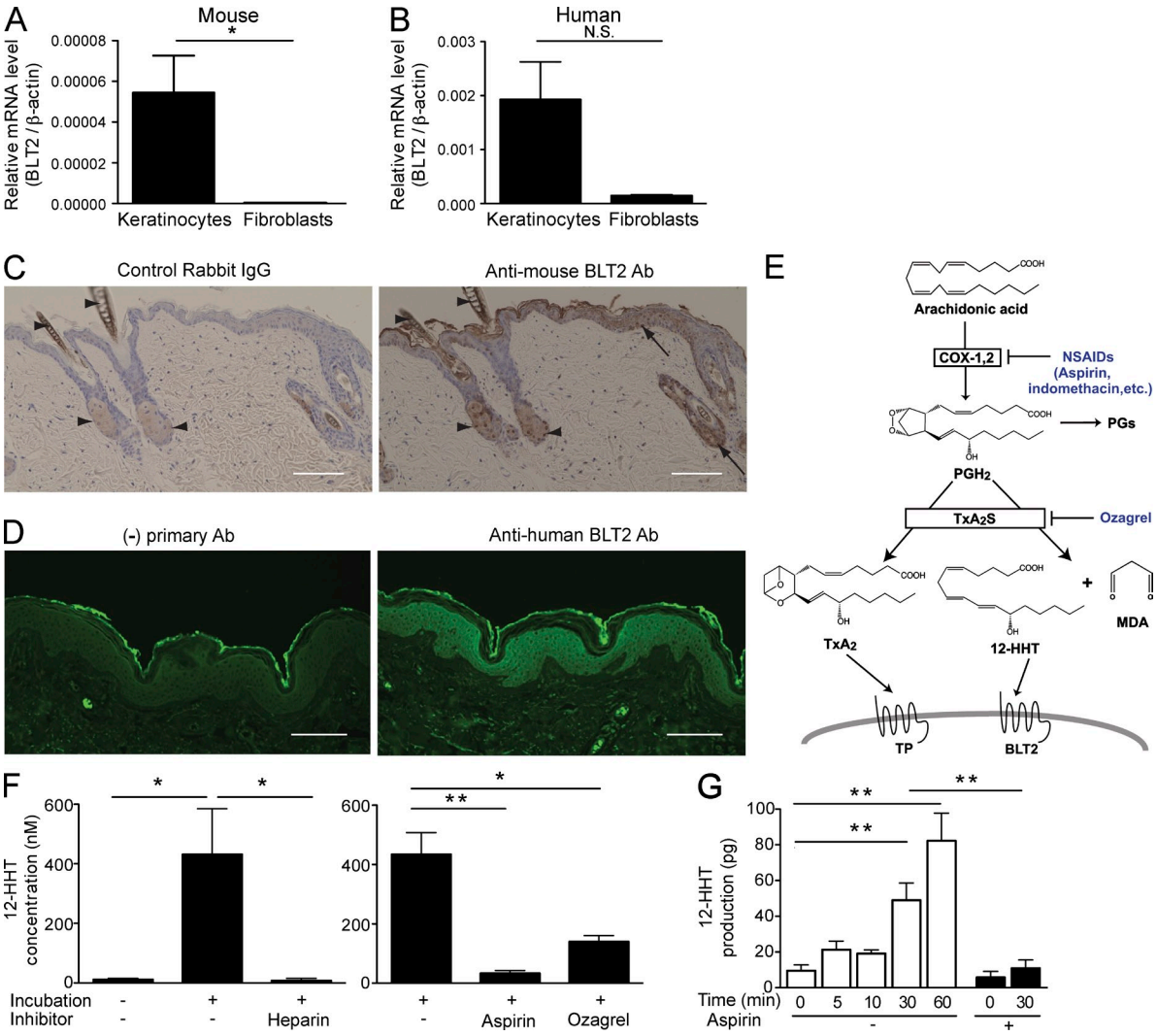

Figure 1. BLT2 is expressed in epidermal keratinocytes, and the ligand 12-HHT is produced in coagulated blood and wound exudate, in a COX/TxA_2S-dependent manner. (A and B) Relative BLT2 mRNA levels were measured by Q-PCR in mouse primary epidermal keratinocytes and dermal fibroblasts (A; $n = 3$ mice per group) and NHEKs and normal human dermal fibroblasts (NHDFs; B; $n = 3$ experimental replicates, $P = 0.16$, unpaired Student's t test). (C) Immunohistochemical staining with anti-mouse BLT2 antibody and control rabbit IgG is shown in normal (uninjured) mouse skin. Arrows, BLT2 signals; arrowheads, nonspecific staining. Bars, 100 µm. (D) Immunohistochemical staining with (right) or without (left) anti-human BLT2 antibody is shown in normal (uninjured) human skin. Bars, 100 µm. (E) Biosynthesis and proposed mechanism of action of 12-HHT. (F and G) 12-HHT was quantified in mouse serum (F) and mouse wound fluid (G) by LC-MS/MS ($n = 3$–5 mice per group). Data represent the mean ± SEM. **, $P < 0.01$; *, $P < 0.05$; N.S., not significant (A and B, unpaired Student's t test; F, one-way ANOVA with Bonferroni post hoc tests; G, two-way ANOVA with Bonferroni post hoc tests). All the results are representative of at least two independent experiments.

(2,4,6-trinitrobenzene sulfonic acid)-induced colitis in mouse (Arita et al., 2005). More investigations are still required to further clarify the roles of lipid mediators in wound healing, especially in regulating keratinocyte migration.

Leukotriene B_4 (LTB_4) is a potent attractant and activator of phagocytic cells, differentiated T cells, and dendritic cells. As such, LTB_4 plays crucial roles in inflammation and immune responses (Luster and Tager, 2004; Mathis et al., 2007). Two G protein–coupled receptors (GPCRs) for LTB_4 were originally cloned in our laboratory. These receptors were designated as the high-affinity LTB_4 receptor BLT1 (Yokomizo et al., 1997) and the low-affinity LTB_4 receptor BLT2 (Kamohara et al., 2000; Yokomizo et al., 2000a). More recently, we identified 12(*S*)-hydroxyheptadeca-5*Z*,8*E*,10*E*-trienoic acid (12-HHT), a downstream metabolite of COX (cyclooxygenase) enzymes, as the endogenous ligand for BLT2 (Okuno et al., 2008). Mouse BLT2 is primarily expressed in epidermal keratinocytes and intestinal tissues (Iizuka et al., 2005), whereas human BLT2 is ubiquitously expressed throughout the body (Kamohara et al., 2000; Yokomizo et al., 2000b). Several lines of evidence suggest that BLT2 participates in DSS (dextran sulfate sodium)–induced colitis (Iizuka et al., 2010), carcinogenesis (Yoo et al., 2004; Hennig et al., 2008), arthritis (Shao et al., 2006), and bronchial asthma (Cho et al., 2010), but

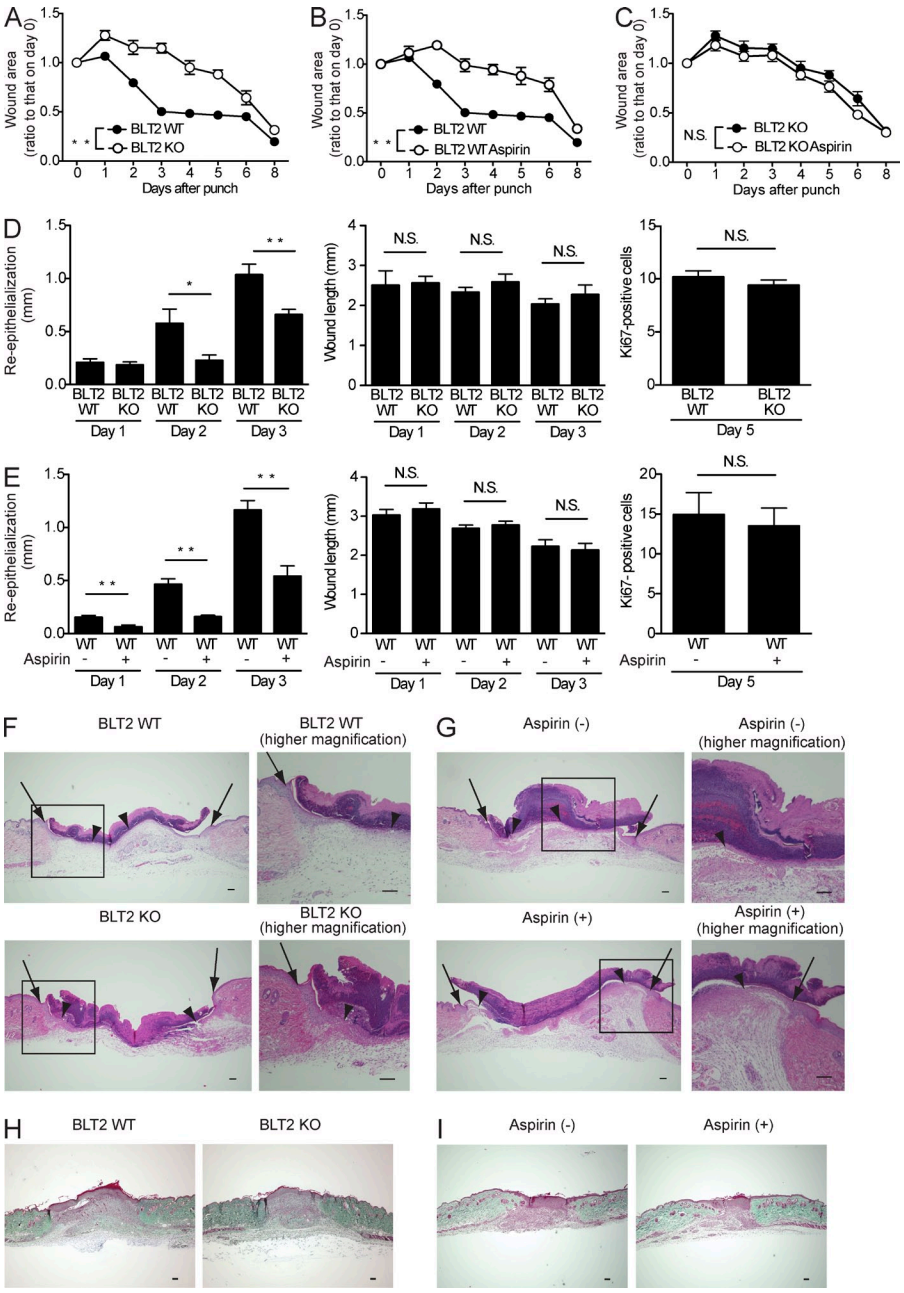

Figure 2. Impairment of the 12-HHT/BLT2 axis delays wound healing and attenuates re-epithelialization in mice. (A–C) Wound closure rate after skin punch in BLT2 WT and BLT2 KO mice with or without aspirin (0.18 mg/ml) in the drinking water (n = 5–6 mice per group). The experiments were performed in parallel. (D and E) Morphometric analyses of wounded skin. Re-epithelialization, wound length, and keratinocyte proliferation (as assessed by Ki67 staining) were evaluated in HE-stained tissue sections from BLT2 WT or BLT2 KO mice (D) and from WT mice with or without aspirin treatment (E) at the indicated days after punch (n = 5 mice per group, two sites per mouse). (F and G) Representative HE-stained sections of the wounds at 3 d after skin punching in BLT2 WT and BLT2 KO mice (F) and in WT mice with or without aspirin treatment (G). Arrows, wound margin; arrowheads, epithelial leading edge. Bars, 100 µm. (H and I) Representative Masson's trichrome–stained sections of the wounds from BLT2 WT and BLT2 KO mice (H, day 5; n = 5 mice per group), control and aspirin-treated WT mice (I, day 5; n = 5 mice per group). Bars, 100 µm. Data represent the mean ± SEM. **, $P < 0.01$; *, $P < 0.05$; N.S., not significant (A–C, two-way ANOVA; D and E, unpaired Student's t test). All the results are representative of at least two independent experiments.

the detailed mechanisms of BLT2 action in vivo are yet to be determined.

Today, aspirin is the best-known of the nonsteroidal anti-inflammatory drugs (NSAIDs). The generally accepted mechanism of high-dose aspirin action is its ability to decrease PG and thromboxane (Tx) production by blocking the activity of COX, which occurs through covalent acetylation of the serine residue in the catalytic pocket of the enzyme. Therefore, aspirin may also inhibit the COX-dependent production of 12-HHT. Aspirin is associated with several recognized clinical benefits, ranging from a reduced risk of heart attack (Group, 1989) and colon polyposis (Chan et al., 2007) to its frequently exploited capacity to alleviate inflammation and pain. However, in addition to its beneficial actions, aspirin (mostly at high doses) triggers serious adverse events (Woodward et al., 2011), the most problematic of which is mucosal injury to the gastrointestinal tract (Awtry and Loscalzo, 2000). Aspirin also delays the onset of labor (Sugimoto et al., 1997) and skin wound healing (Pollack, 1984; McGrath and Breathnach, 2004; Kaushal et al., 2007). However, the precise mechanisms responsible for the aspirin-related delay in wound healing are as yet wholly unknown.

The current study therefore investigated the role of the 12-HHT/BLT2 axis in regulating keratinocyte migration both in vivo and in vitro, and consequently revealed a novel mechanism underlying the aspirin-dependent delay in wound

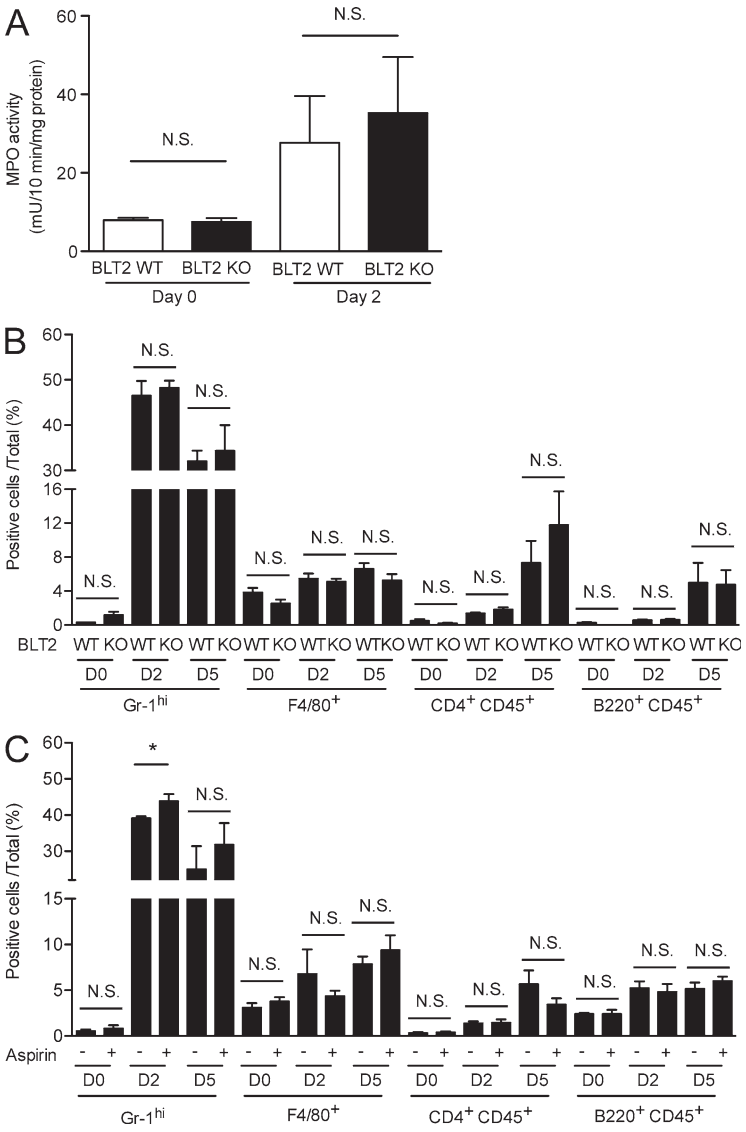

Figure 3. Skin inflammation is not affected by BLT2 deficiency or aspirin treatment. (A) MPO activity in homogenates of punched skin obtained from BLT2 WT and BLT2 KO mice ($n = 3$ mice per group). Punch biopsies (5 mm in diameter) were obtained at 2 d after skin punching and used for the assay. (B and C) Frequency of immune cells expressing the indicated surface markers as determined by flow cytometry analysis in the punched skin of BLT2 WT and BLT2 KO mice (B, $n = 3$ mice per group) and WT mice with or without aspirin treatment (C, $n = 3$ mice per group). Aspirin treatment (0.18 mg/ml in the drinking water) was initiated at 2 d before skin punching. Punch biopsies (5 mm in diameter) were obtained at 2 and 5 d after skin punching and used for the assay. Data represent the mean ± SEM. *, $P < 0.05$, N.S., not significant (unpaired Student's *t* test). All the results are representative of at least two independent experiments.

healing. Most importantly, the results presented herein provide a promising new therapeutic approach for the treatment of intractable ulcers.

RESULTS

Expression of BLT2 in keratinocytes and the production of 12-HHT

To determine the cells that express BLT2 in skin, we performed a quantitative reverse transcription polymerase chain reaction (Q-PCR) analysis along with immunohistochemical staining to investigate BLT2 expression in skin cells and intact skin, respectively. BLT2 mRNA was prominently detected in both mouse and human epidermal keratinocytes, but not in dermal fibroblasts (Fig. 1, A and B). Immunohistochemical staining revealed that BLT2 was mainly expressed in the epidermal layer of normal (uninjured) mouse and human skin (Fig. 1 C and D).

A BLT2 ligand, 12-HHT, is produced from arachidonic acid by the actions of COX and thromboxane A_2 synthase (TxA_2S; Fig. 1 E; Hamberg et al., 1974). To determine whether 12-HHT is generated during skin wound healing, we quantified 12-HHT in mouse serum and wound exudate by using liquid chromatography-tandem mass spectrometry (Kita et al., 2005; Matsunobu et al., 2013). A large amount of 12-HHT was produced during blood coagulation, and its production was inhibited by the anticoagulant heparin (Fig. 1 F, left). Both aspirin and ozagrel, a TxA_2S inhibitor, inhibited 12-HHT production during blood coagulation (Fig. 1 F, right). After skin punching, 12-HHT was released into the wound fluid, and its concentration increased in a time-dependent manner. However, aspirin administration again inhibited 12-HHT accumulation (Fig. 1 G). These results indicate that the 12-HHT/BLT2 axis may play some roles in skin wound healing.

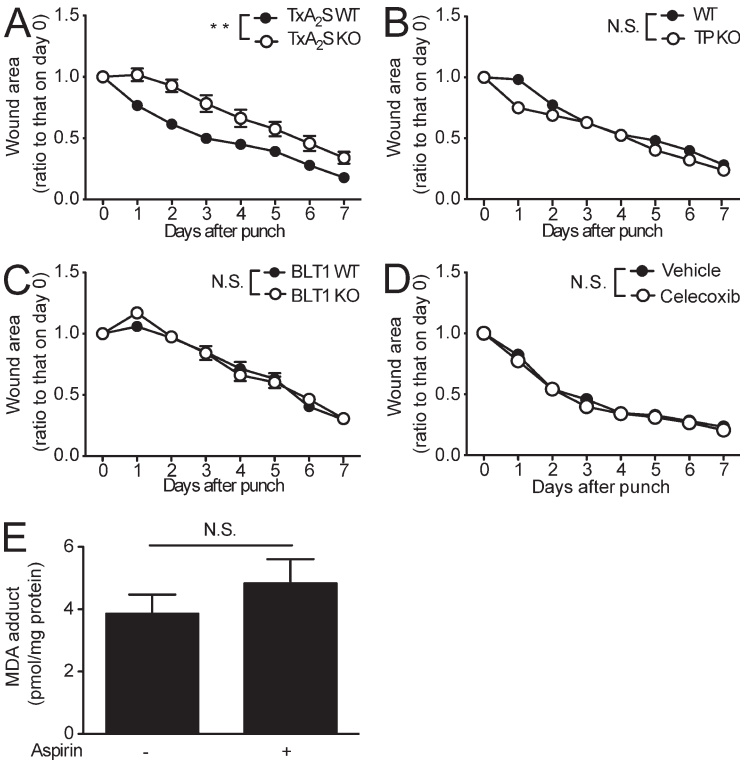

Figure 4. The TxA_2/TP axis and BLT1 are not involved in wound healing. (A–D) Wound closure rate in TxA_2S WT and TxA_2S KO mice (A, *n* = 5–6 mice per group), WT and TP KO mice (B, *n* = 5 mice per group), BLT1 WT and BLT1 KO mice (C, *n* = 5 mice per group), and vehicle and celecoxib-treated WT mice (D, *n* = 6–7 mice per group). In D, vehicle (0.5% methyl cellulose) or celecoxib (25 mg/kg body weight) was administrated by gavage to the mice (male C57BL/6J, 8 wk old) every day. Celecoxib treatment started 48 h before skin punching. (E) MDA adduct levels were measured in mouse skin samples from WT mice with or without aspirin treatment (*n* = 4 mice per group). Aspirin treatment (0.18 mg/ml in the drinking water) was initiated at 2 d before the biopsy. A 5-mm punch biopsy sample was used to assess the presence of MDA adducts via ELISA. Data represent the mean ± SEM. **, $P < 0.01$; N.S., not significant (A–D, two-way ANOVA; E, unpaired Student's *t* test). All the results are representative of at least two independent experiments.

Impairment of the 12-HHT/BLT2 axis delays skin wound healing due to attenuated re-epithelialization

We next determined the impact of BLT2 deficiency and/or aspirin treatment on skin wound healing in vivo. Full-thickness 3-mm punch biopsy wounds were made in the dorsal skin of BLT2 WT and BLT2 KO mice with or without aspirin treatment. The wound closure rate was then assessed via daily measurement of the wound area for 8 d, and the kinetics of wound closure were evaluated as percentage of original wound areas (Fig. 2, A–C). BLT2 KO mice exhibited significantly delayed wound closure compared with BLT2 WT mice (Fig. 2 A). Aspirin treatment (at a therapeutic high dose of 0.18 mg/ml in the drinking water) significantly delayed wound closure only in BLT2 WT mice (Fig. 2 B), but no further effects were observed in BLT2 KO mice in response to aspirin administration (Fig. 2 C).

Detailed morphometric analyses of punched skin tissues were next performed on HE-stained sections. No apparent structural differences were found in the HE-stained intact skin of BLT2 WT versus BLT2 KO mice at the light microscopy level (unpublished data). After injury, re-epithelialization and wound contraction are important processes that control the overall rate of repair. We observed that re-epithelialization (determined by measuring the lengths of the wounds within the neoepithelium) was impaired in BLT2 KO mice (Fig. 2, D and F) and aspirin-treated WT (Fig. 2, E and G), whereas wound length (determined by measuring the lengths between the wound margins) was unaffected (Fig. 2, D and E, middle). In addition, keratinocyte proliferation (evaluated by counting Ki67-positive cells) were also unaffected by BLT2 deficiency (Fig. 2 D, right) or aspirin administration (Fig. 2 E, right). Because fibroblasts are also a crucial component of wound healing by enhancing wound contraction, collagen deposition in wound tissue was evaluated by Masson's trichrome staining. The results showed that neither BLT2 deficiency nor aspirin treatment affected collagen deposition during wound healing (Fig. 2, H and I). The delayed skin wound healing brought about by BLT2 deficiency and aspirin treatment was not due to a modified immune response because skin inflammation (evaluated by measuring myeloperoxidase [MPO] activity in the skin [Fig. 3 A], as well as by flow cytometry analysis of the immune cells [Fig. 3, B and C]) was unaltered. Given that BLT2 is expressed in keratinocytes but not in dermal fibroblasts (Fig. 1, A–D), we hypothesized that the 12-HHT/BLT2 axis enhances re-epithelialization by accelerating keratinocyte migration during wound healing.

Because aspirin treatment inhibits both 12-HHT and TxA_2 production (Fig. 1 E), reduced TxA_2 levels might also be involved in the deleterious effects of aspirin. To investigate this hypothesis, we performed a punch assay in the dorsal skin of mice lacking TxA_2S, the terminal enzyme required for the production of TxA_2 and 12-HHT, and mice lacking the TxA_2 receptor (TP). TxA_2S deficiency delayed wound closure (Fig. 4 A), whereas wound closure was normal in TP KO mice (Fig. 4 B). These findings indicate that a reduction in TxA_2 is not responsible for the aspirin-dependent delay in skin wound healing. Wound closure was also normal in mice deficient in BLT1 (Yokomizo et al., 1997), a high-affinity

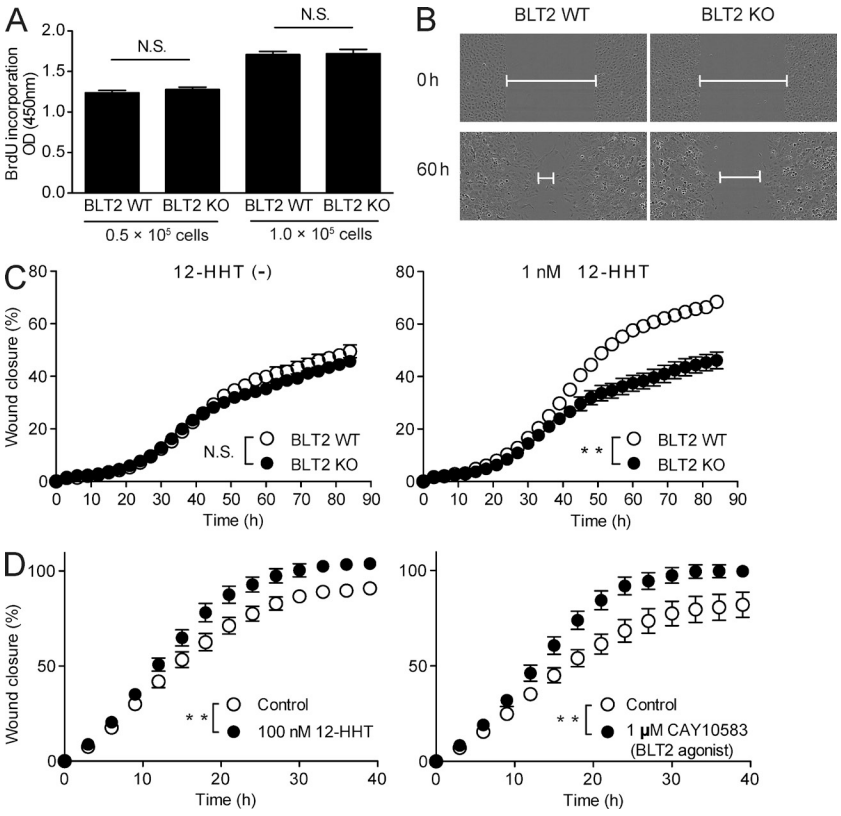

Figure 5. 12-HHT and a synthetic BLT2 agonist enhance primary keratinocyte migration. (A) BrdU incorporation was assessed in primary epidermal keratinocytes obtained from WT and BLT2 KO mice (n = 5 mice per group). (B–D) Keratinocytes were cultured to confluency, mechanically wounded by scratching, and then incubated in medium containing the indicated reagents. (B) Representative fields show the wound gap filled by WT and BLT2 KO primary keratinocytes cultured in the presence of 1 nM 12-HHT at 0 and 60 h after scratching. Lines indicate remaining gap. (C and D) Quantification of mouse primary keratinocyte (C, n = 9 experimental replicates) and NHEK (D, n = 12 experimental replicates) migration. Data represent the mean ± SEM. **, $P < 0.01$; N.S., not significant (A, unpaired Student's t test; C and D, two-way ANOVA). All the results are representative of at least two independent experiments.

LTB_4 receptor (Fig. 4 C), also ruling out the involvement of BLT1 in wound healing. The effect of a COX2 selective inhibitor, celecoxib, on wound healing was also studied. Celecoxib treatment (25 mg/kg body weight) had no effect on wound closure in WT mice (Fig. 4 D). We also measured 12-HHT production in both mouse serum and wound fluid, which was not affected by celecoxib treatment (unpublished data).

Malondialdehyde (MDA) is also generated with TxA_2 and 12-HHT by TxA_2S from PGH_2 (Fig. 1 E), as well as by the peroxidation of various lipids (Esterbauer et al., 1991). We next explored the influence of aspirin on MDA adduct content in the WT mouse skin. Aspirin treatment did not reduce the level of MDA (Fig. 4 E). Hence, diminished MDA production does not contribute to the aspirin-mediated delay in wound closure. Collectively, the current observations suggest that a decrease in 12-HHT levels is responsible for the aspirin-dependent delay in skin wound healing.

The 12-HHT/BLT2 axis accelerates keratinocyte migration independently of cell proliferation

To assess the role of the 12-HHT/BLT2 axis in keratinocyte migration during wound repair, an in vitro scratch assay was performed by using mouse and human primary keratinocytes. BLT2 deficiency did not affect primary keratinocyte proliferation (Fig. 5 A). Furthermore, in the absence of 12-HHT (Fig. 5 C, left), the wound closure rate was similar between BLT2 WT and BLT2 KO keratinocytes. However, BLT2 WT keratinocytes exhibited enhanced migration in the presence of 1 nM 12-HHT, whereas BLT2 KO keratinocytes did not (Fig. 5, B and C, right; Videos 1 and 2). This finding was confirmed in normal human epidermal keratinocytes (NHEKs). Both 12-HHT and a synthetic BLT2 agonist, CAY10583 (Iizuka et al., 2005), significantly enhanced NHEK migration relative to control, untreated cells (Fig. 5 D).

To analyze the detailed mechanisms behind the participation of the 12-HHT/BLT2 axis in cell migration, we next examined the effect of BLT2 overexpression on the migration of HaCaT cells (a human keratinocyte cell line) that do not endogenously express functional BLT2. Stable overexpression of BLT2 was confirmed by flow cytometry (Fig. 6 A), and BLT2 overexpression had no effect on cell proliferation (Fig. 6 B). Either BLT2 overexpression or 12-HHT treatment did not promote resistance to cell death both in HaCaT-mock and HaCaT-BLT2 cells during scratch assay (Fig. 6 C). In contrast, HaCaT-BLT2 cells migrated faster than HaCaT-mock cells in the presence of 0.5% FCS that contains ∼0.75 nM 12-HHT (Kita et al., 2005; Matsunobu et al., 2013; Fig. 6, D and E; Videos 3 and 4). Moreover, the BLT2 antagonist LY255283 (Yokomizo et al., 2001) inhibited the migration of HaCaT-BLT2 cells, but not HaCaT-mock cells (Fig. 6 F). Conversely, both 12-HHT and a BLT2 agonist accelerated the migration of HaCaT-BLT2 cells in the absence of FCS but had no effect on HaCaT-mock cells (Fig. 6, G and H). Furthermore, mitomycin C treatment, which inhibits cell proliferation, did

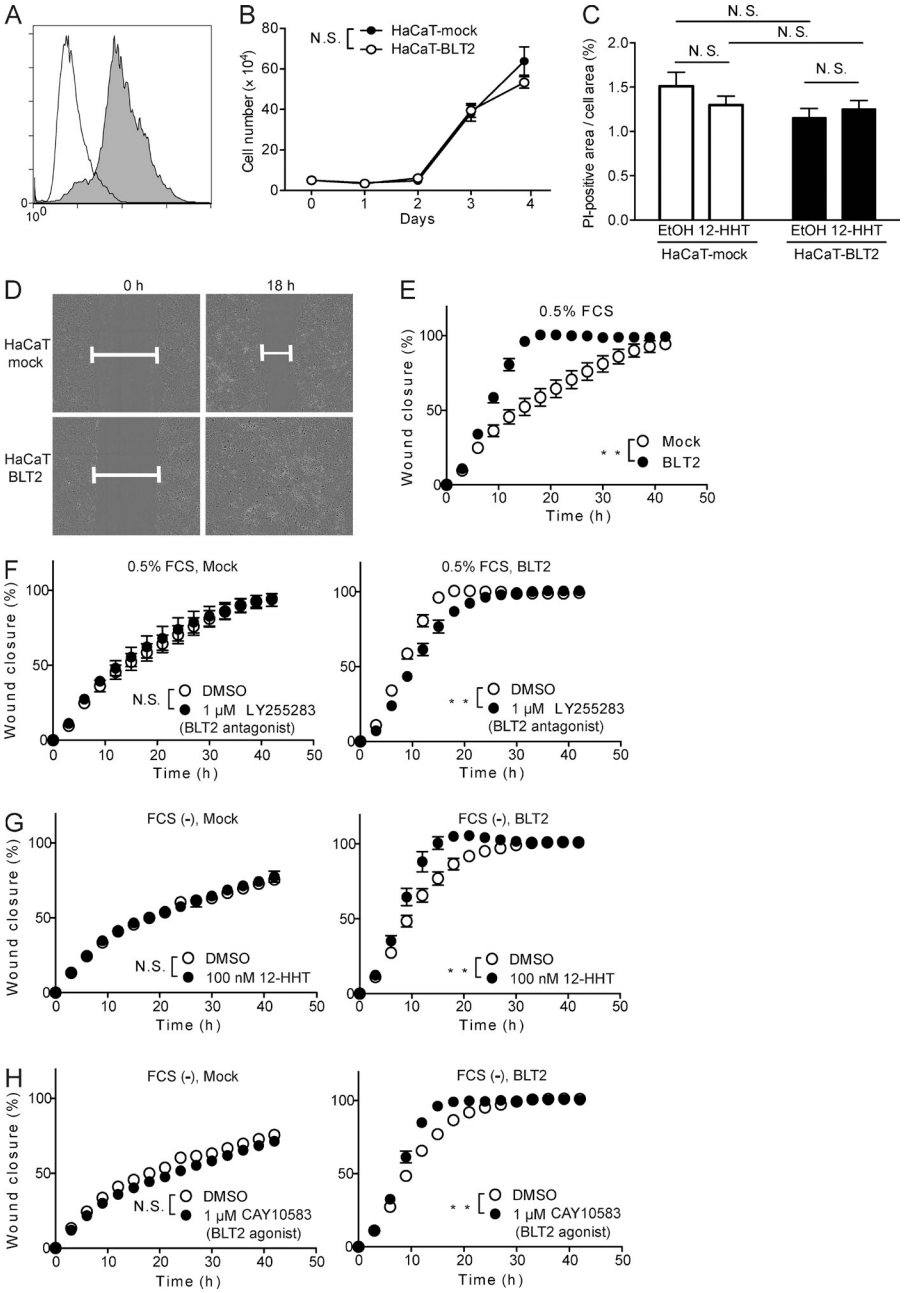

Figure 6. 12-HHT and a synthetic BLT2 agonist enhance HaCaT-BLT2 cell migration. (A) Flow cytometry analysis of HaCaT cells stably expressing Flag-tagged BLT2 (gray) and HaCaT-mock transfectants (white) after staining with anti-Flag antibody. (B) Growth of HaCaT-mock and HaCaT-BLT2 cells ($n = 3$ experimental replicates). (C) Quantification of cell death of HaCaT-mock and HaCaT-BLT2 cells by propidium iodide (PI) staining 12 h after scratching. Cells were cultured in medium containing EtOH or 100 nM 12-HHT ($n = 3$–4 experimental replicates). (D) Representative fields show the wound gap filled by HaCaT-mock and HaCaT-BLT2 cells cultured in medium containing 0.5% FCS at 0 h and 18 h. (E–H) Quantification of HaCaT-mock and HaCaT-BLT2 cell migration ($n = 4$ experimental replicates). The cells were cultured in medium containing 0.5% FCS (E and F) or in FCS-free medium (G and H) containing the synthetic BLT2 antagonist LY255283 (F), 12-HHT (G), or the synthetic BLT2 agonist (H). Data represent the mean ± SEM. **, $P < 0.01$; N.S., not significant (B and E–H, two-way ANOVA; C, two-way ANOVA with Bonferroni post hoc tests). All the results are representative of at least two independent experiments.

not alter BLT2-dependent cell migration (unpublished data). Thus, the 12-HHT/BLT2 axis accelerates keratinocyte migration in vitro independently of cell proliferation and cell death.

TNF and MMP9 participate in 12-HHT/BLT2-dependent keratinocyte migration

To gain insight into the molecular mechanism by which the 12-HHT/BLT2 axis stimulates keratinocyte migration, we investigated global transcription in mouse skin by DNA microarray analysis. Total RNA was isolated from the skin of BLT2 WT and BLT2 KO mice at 2 d after skin punching or without skin punching. The RNA was then evaluated for its content of injury-related transcripts. The analysis revealed that injury-related cytokines, chemokines, and MMPs, which are reported to enhance keratinocyte migration (Gillitzer and Goebeler, 2001; Kyriakides et al., 2009), were down-regulated in uninjured BLT2 KO mouse skin (data deposited to GEO repository under accession no. GSE53400). Q-PCR confirmed that the mRNA levels of TNF, IL-1β, and MMP9 were significantly lower in the uninjured skin of BLT2 KO mice than those in BLT2 WT mice, and these transcripts were all up-regulated after skin punching in both groups (Fig. 7 A). Consistent with these observations, the transcription levels of TNF, IL-1β, and MMP9 were up-regulated in 12-HHT–treated HaCaT-BLT2 cells (Fig. 7 B). Interestingly, 12-HHT initially

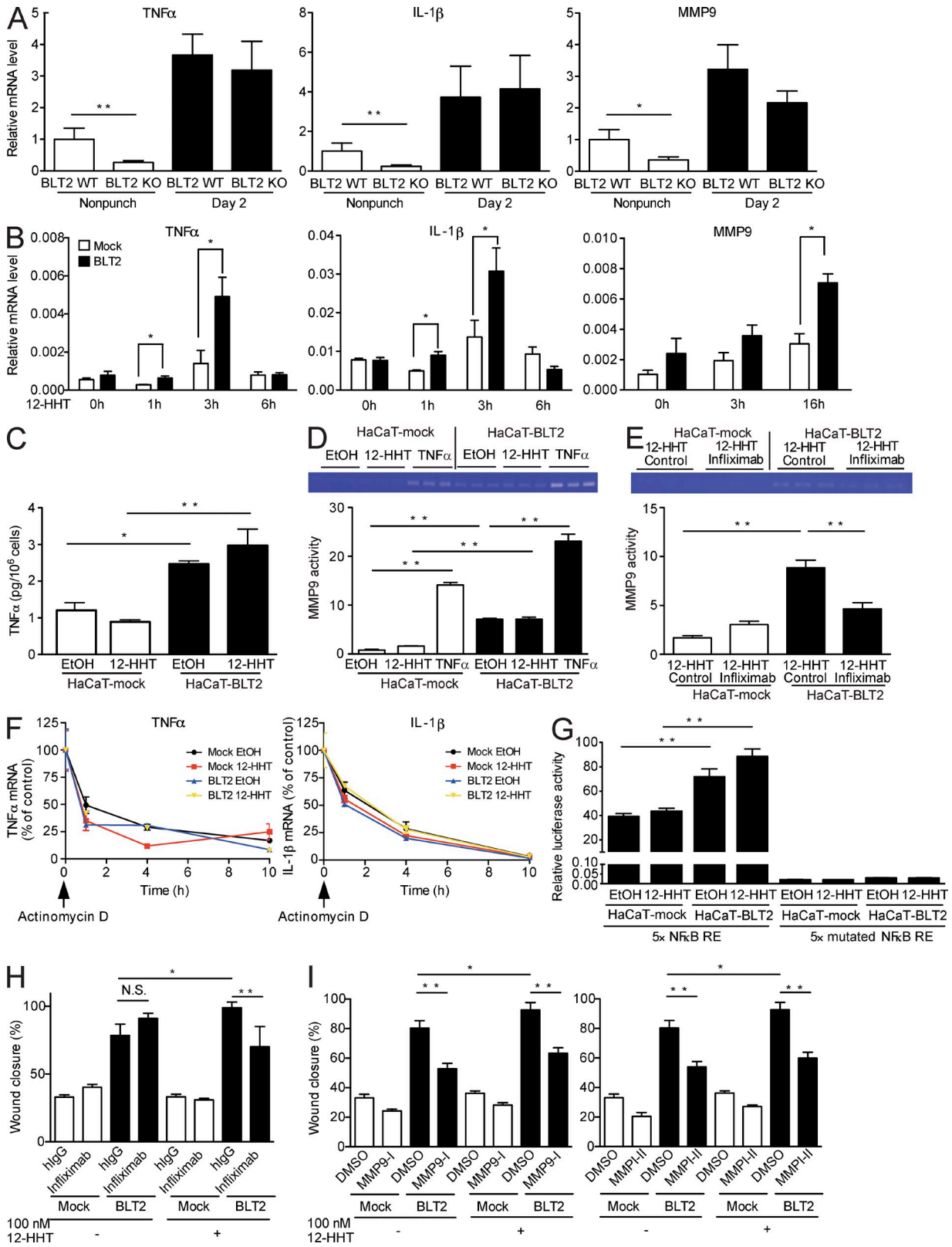

Figure 7. TNF and MMP9 participate in 12-HHT/BLT2–dependent HaCaT cell migration. (A) Relative levels of TNF, IL-1β, and MMP9 mRNA were measured by Q-PCR in BLT2 WT and BLT2 KO mouse skin (n = 3–7 mice per group). Punch biopsies (5 mm in diameter) were obtained at 2 d after skin punching and used for the assay. The relative mRNA level in uninjured BLT2 WT mice was set as 1. (B) HaCaT-mock and HaCaT-BLT2 cells were stimulated with 1 µM 12-HHT, and the relative levels of TNF, IL-1β, and MMP9 mRNA were measured by Q-PCR (n = 3 experimental replicates). (C) HaCaT-mock and

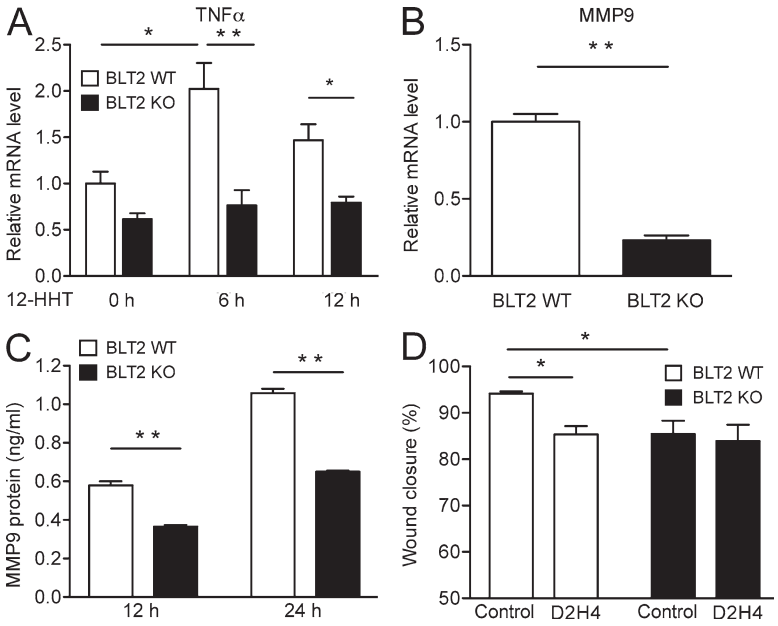

Figure 8. TNF and MMP9 participate in 12-HHT/BLT2–dependent mouse primary keratinocyte migration. (A) Relative mRNA levels of TNF were measured by Q-PCR in BLT2 WT and BLT2 KO mouse primary keratinocytes. Cells were stimulated with 100 nM 12-HHT for the indicated time ($n = 4$ experimental replicates). The relative mRNA level in unstimulated BLT2 WT keratinocytes was set as 1. (B) Relative levels of MMP9 mRNA were measured by Q-PCR in BLT2 WT and BLT2 KO mouse primary keratinocytes ($n = 4$ experimental replicates). The relative mRNA level in BLT2 WT keratinocytes was set as 1. (C) Mouse MMP9 protein levels in the culture medium of mouse primary keratinocytes were measured by ELISA after 12 and 24 h of culture ($n = 4$ experimental replicates). (D) The effect of mouse TNF neutralizing antibody D2H4 on the migration of BLT2 WT and BLT2 KO mouse primary keratinocytes. Cells were cultured in medium containing 1 nM 12-HHT and 10 ng/ml control IgG or 10 ng/ml D2H4 for 39 h ($n = 5$–6 experimental replicates). Data represent the mean ± SEM. **, $P < 0.01$; *, $P < 0.05$ (A and D, two-way ANOVA with Bonferroni post hoc tests; B and C, unpaired Student's *t* test). All the results are representative of at least two independent experiments.

induced expression of TNF and IL-1β mRNA, followed somewhat later by MMP9 mRNA, suggesting that MMP9 transcription occurs downstream of TNF and IL-1β transcription.

In agreement with the Q-PCR data, increases in TNF protein levels (Fig. 7 C) and MMP9 activity (Fig. 7 D) were detected in the culture supernatant of HaCaT-BLT2 cells. Based on previous reports showing that TNF induces MMP9 transcription (Holvoet et al., 2003; Scott et al., 2004), we next studied the relationship between TNF and MMP9. MMP9 activity in HaCaT-BLT2 cells was increased by TNF stimulation (Fig. 7 D) and decreased when the cells were incubated with Infliximab, a human TNF-neutralizing antibody (Fig. 7 E). Hence, these results show that the 12-HHT/BLT2 axis upregulates MMP9 activity via augmentation of TNF secretion.

Neither BLT2 expression nor 12-HHT stimulation had any effect on the stability of TNF or IL-1β mRNA (Fig. 7 F), suggesting that the 12-HHT/BLT2 axis enhances TNF and IL-1β expression at the transcriptional level. As the transcription of both TNF and IL-1β is driven by NF-κB (Cogswell et al., 1994; Kuprash et al., 1999), we next investigated whether BLT2 can stimulate NF-κB activity. Reporter gene analysis showed that NF-κB activity was higher in HaCaT-BLT2 cells than in HaCaT-mock cells, and that NF-κB activity in HaCaT-BLT2 cells was further enhanced by 12-HHT (Fig. 7 G, left). Basal and 12-HHT–dependent NF-κB activities were completely lost by mutating all the NF-κB responsive elements (REs) in the reporter plasmid (Fig. 7 G, right).

To clarify the involvement of TNF and MMP9 in keratinocyte migration, the effects of Infliximab and two MMP inhibitors were examined in a wound scratch assay. As expected, Infliximab significantly reduced the migration of HaCaT-BLT2 cells only in the presence of 12-HHT (Fig. 7 H). The MMP9 specific inhibitor (MMP9-I) and a broad MMP inhibitor (MMPI-II) markedly reduced the migration of HaCaT-BLT2 cells and slightly reduced the migration of HaCaT-mock cells both in the presence and absence of 12-HHT, indicating that MMPs might control keratinocyte migration in both 12-HHT/BLT2/TNF–dependent and –independent pathways (Fig. 7 I).

The involvement of TNF and MMP9 in cell migration was also investigated in mouse primary keratinocytes isolated from BLT2 WT and BLT2 KO mice. 12-HHT significantly

HaCaT-BLT2 cells were stimulated with EtOH vehicle or 1 µM 12-HHT for 6 h, and TNF protein levels were assessed in the culture medium ($n = 3$ experimental replicates). (D and E) MMP9 activity in the culture medium was measured by zymography. HaCaT-mock and HaCaT-BLT2 cells were serum-starved for 3 h and then stimulated for 24 h with EtOH vehicle, 1 µM 12-HHT, or 10 ng/ml TNF (D, $n = 3$ experimental replicates), or with 1 µM 12-HHT and 100 µg/ml control IgG or 100 µg/ml Infliximab (E, $n = 3$ experimental replicates). (F) Determination of TNF and IL-1β mRNA stability in HaCaT-mock and HaCaT-BLT2 cells. The cells were cultured in medium containing 5 µg/ml actinomycin D and EtOH vehicle or 1 µM 12-HHT and then harvested at the indicated times. TNF and IL-1β mRNA levels were quantified by Q-PCR ($n = 3$ experimental replicates). (G) Determination of NF-κB activity in HaCaT-mock and HaCaT-BLT2 cells. Cells were stimulated with EtOH vehicle or 1 µM 12-HHT, and subjected to the dual luciferase assay ($n = 3$ experimental replicates). (H and I) Quantification of cell migration of HaCaT-mock and HaCaT-BLT2 cells at 15 h after scratching. Cells were cultured in serum-free medium without 12-HHT or with 100 nM 12-HHT, and control IgG or 100 µg/ml Infliximab (H, $n = 5$–8 experimental replicates); or DMSO and 10 µM MMP9 inhibitor I (I, left, $n = 6$–8 experimental replicates) or 10 µM MMP inhibitor II (I, right, $n = 6$–10 experimental replicates). Data represent the mean ± SEM. **, $P < 0.01$; *, $P < 0.05$ (A and B, unpaired Student's *t* test; C–E and G–I, two-way ANOVA with Bonferroni post hoc tests). All the results are representative of at least two independent experiments.

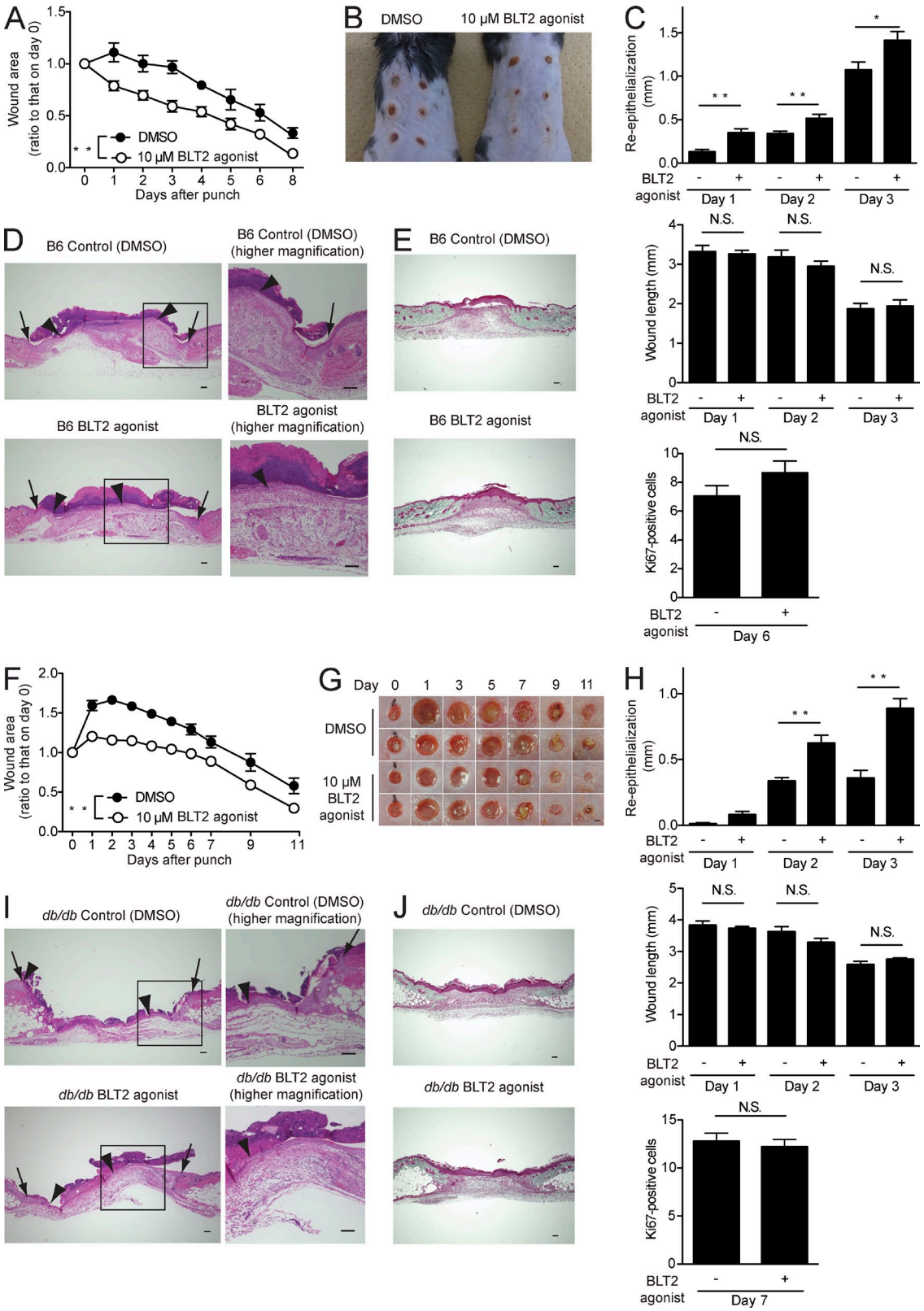

Figure 9. A synthetic BLT2 agonist accelerates wound healing and enhances re-epithelialization in C57BL/6J and *db/db* mice. DMSO vehicle or a synthetic BLT2 agonist (10 μM in Vaseline) was applied daily to the skin wounds of C57BL/6J (B6) mice (A–E) and *db/db* mice (F–J). (A and F) Wound closure rate in C57BL/6J (A, *n* = 3 mice per group) and *db/db* (F, *n* = 8–10 mice per group) mice. (B and G) Gross appearance of the wounds in C57BL/6J mice on day 6 (B, *n* = 3 mice per group) and *db/db* mice at the indicated days (G, *n* = 8–10 mice per group). Bar, 1 mm. (C and H) Morphometric analysis

up-regulated the transcription of TNF only in BLT2 WT keratinocytes but not in BLT2 KO keratinocytes (Fig. 8 A). Both MMP9 mRNA (Fig. 8 B) and MMP9 protein levels (Fig. 8 C) were significantly higher in BLT2 WT keratinocytes. The mouse TNF-neutralizing antibody D2H4 only reduced the migration of BLT2 WT keratinocytes (Fig. 8 D). Collectively, these results clearly indicate that the 12-HHT/BLT2 axis accelerates keratinocyte migration by stimulating NF-κB signaling, which then induces the expression of TNF and MMP9 to promote wound healing.

A BLT2 agonist accelerates wound healing and enhances re-epithelialization

Finally, to address the clinical relevance of our observations, the therapeutic effects of a BLT2 agonist were determined on wound healing in C57BL/6J and *db/db* mice. The *db/db* mouse is an animal model of diabetes and exhibits impaired wound closure (Greenhalgh et al., 1990). Topical application of a BLT2 agonist accelerated wound closure by enhancing re-epithelialization in both C57BL/6J mice (Fig. 9, A–E) and *db/db* mice (Fig. 9, F–J) but not by promoting contraction (Fig. 9, C [middle] and H [middle]), keratinocyte proliferation (Fig. 9, C [bottom] and H [bottom]), or collagen deposition (Fig. 9, E and J). Furthermore, a BLT2 agonist did not influence skin inflammation either (unpublished data). Thus, BLT2 activation in keratinocytes accelerates wound healing by enhancing keratinocyte migration.

DISCUSSION

Our findings suggest that impairment of the 12-HHT/BLT2 axis attenuated epidermal keratinocyte migration, thereby contributing to delayed re-epithelialization during wound healing. Furthermore, aspirin, the most commonly used NSAID, retards skin wound healing by inhibiting the production of 12-HHT, an endogenous ligand for BLT2. Our study also suggests the use of BLT2 agonists as therapeutic agents to accelerate wound healing, particularly for intractable wounds.

Wound healing proceeds via sequential yet overlapping phases, including hemostatic, inflammatory, proliferative, and remodeling phases (Martin, 1997; Baum and Arpey, 2005). Underlying these events are numerous, complex processes involving various cells, regulatory factors, and components of the extracellular matrix. Two distinct cellular mechanisms directly lead to the closure of a wound (Coulombe, 2003). One is a re-epithelialization event, achieved through a combination of enhanced migration and mitosis of keratinocytes in the epidermis proximal to the wound margin. The other is a fibroblast-mediated centripetal contraction of the wound site, pulling the edges of the wound closer together (Coulombe, 2003). All stages of injury repair are controlled by a wide variety of growth factors, cytokines, and lipid mediators. Although much has been learned about the effects of growth factors (e.g., platelet-derived growth factor [PDGF], TGF-β, and fibroblast growth factor 2) on the repair process (Werner and Grose, 2003), next to little is known about the role of lipid mediators. Many lipid mediators are abundant in the skin and biologically active. Our data now clearly show the beneficial actions of 12-HHT, a COX/TxA_2S-dependent fatty acid, on wound healing via stimulation of the BLT2 receptor to promote keratinocyte migration.

The complexity of wound healing is certainly rivaled in magnitude by its medical and social importance. Defects in skin wound repair that occur secondary to pathophysiological conditions, such as diabetes, peripheral neuropathy, pressure, and venous stasis, all contribute critically to health care–related expenses (Falanga et al., 1994; Singer and Clark, 1999). Hence, research directed toward better understanding the fundamentals of the homeostatic wound closure response is urgently required. However, the rather discouraging clinical results of local application of growth factors made clear that the biology of wound healing is much more complicated than initially assumed, necessitating consideration of additional components and mechanisms (Gillitzer and Goebeler, 2001; Fu et al., 2005). To date, only a single recombinant growth factor, recombinant human PDGF-BB (rhPDGF-BB), has been approved for use in skin wound repair by the US Food and Drug Administration; moreover, its usage is limited to the management of diabetic foot ulcers (Fang and Galiano, 2008). PDGF accelerates wound healing by stimulating fibroblast proliferation, in addition to the induction of the myofibroblast phenotype (Werner and Grose, 2003).

Growth factors and extracellular matrix signals are almost assuredly not the only relevant influences on wound closure, and many other biologically active mediators are thought to have a significant impact on wound healing. Recently, new therapeutic agents that directly improve the re-epithelialization process have attracted great interest. The re-epithelialization process begins within several hours after injury and, given its role in the restoration of an intact epidermal barrier, is absolutely essential for optimal wound closure. The directed migration of keratinocytes is in turn essential for re-epithelialization, and defects in this function are associated with chronic nonhealing wounds, such as diabetic ulcers (Stojadinovic et al., 2005). Diabetic patients frequently suffer from severely impaired wound healing, with a lifetime risk of 15% for developing diabetic skin ulcerations. Diabetic ulcers have a poor prognosis, and 15–27% of all diabetic ulcers lead to the surgical removal of bone (Jeffcoate and Harding, 2003). Notably,

of wounded skin. Re-epithelialization (top), wound length (middle), and Ki67-positive keratinocyte proliferation (bottom; $n = 5$ mice per group, two sites per mouse) were evaluated in HE-stained tissue sections. (D and I) Representative HE-stained sections of the wounds at 3 d after skin punching. Arrows, wound margin; arrowheads, epithelial leading edge. Bars, 100 µm. (E and J) Representative Masson's trichrome–stained sections of the wounds (E, day 6; J, day 7; $n = 5$ mice per group). Bars, 100 µm. Data represent the mean ± SEM. **, $P < 0.01$; *, $P < 0.05$; N.S., not significant (A and F, two-way ANOVA; C and H, unpaired Student's *t* test). All the results are representative of at least two independent experiments.

the migration and proliferation of keratinocytes are greatly reduced at the nonhealing edge of diabetic wounds (Stojadinovic et al., 2005; Brem and Tomic-Canic, 2007).

Our results revealed that activation of BLT2 by a specific agonist significantly accelerated re-epithelialization in *db/db* mice (Fig. 9). This favorable effect on wound closure was due to enhanced keratinocyte migration during the healing process. Nonetheless, it is highly unlikely that a single growth factor, such as PDGF, will be able to resolve all issues of repair or strengthen all vulnerabilities of chronic wounds. A combination of therapeutic approaches is more likely to culminate in a successful treatment outcome, especially in the case of chronic or intractable wounds.

To this end, the use of platelet-rich gels has recently been suggested to accelerate wound healing (Borzini and Mazzucco, 2005; Demidova-Rice et al., 2012). Activated platelets produce several growth factors and lipid mediators, which, as described above, participate in all phases of wound healing (Werner and Grose, 2003). According to our findings, 12-HHT generated during blood coagulation (Fig. 1 F) may be one of the more efficacious components of platelets, in addition to various PDGFs and cytokines thought to improve wound healing. Our study also suggests the therapeutic use of BLT2 agonists in promoting wound healing via enhancement of keratinocyte migration. This approach may be of particular interest in the clinical treatment of intractable diabetic ulcers and bedsores.

Many factors control the efficacy, speed, and manner of wound healing and are divided into two types, local and systemic factors. Aspirin is included on the list of systemic factors that inhibit wound repair (Pollack, 1984; McGrath and Breathnach, 2004). However, the mechanisms of the aspirin-dependent delay in wound healing were formerly unknown. 12-HHT, a COX/TxA_2S-derived fatty acid, was long considered to be merely a by-product of TxA_2 generation until our identification of this fatty acid as an endogenous high-affinity ligand for BLT2 (Okuno et al., 2008). Notably, aspirin (at its therapeutic high dose) down-regulates 12-HHT production during blood coagulation (Fig. 1 F) and in wound fluid (Fig. 1 G), revealing for the first time that a reduction in 12-HHT levels is responsible, at least in part, for the aspirin-mediated hindrance to wound closure. Indomethacin, another well-known NSAID, also inhibited 12-HHT production in mouse serum and delayed wound closure (unpublished data), showing that the adverse effect on wound repair is not specific to aspirin. The main origin of 12-HHT during skin wound healing in our study is presumably activated platelets, in which COX1 is the dominant isoform (Seta et al., 2009). Importantly, our findings are strongly supported by the expression of BLT2 in human and mouse epidermal keratinocytes (Fig. 1, A–D). In addition, a time-dependent accumulation of 12-HHT in the wound exudate (Fig. 1 G) suggests the requirement of 12-HHT during the repair process.

Aspirin is a unique NSAID; at a high dose, which was used in this study, its actions are thought to stem from the total inhibition of both cyclooxygenase and lipoxygenase activities of COXs. In contrast, at lower doses, aspirin initiates the biosynthesis of novel anti-inflammatory mediators from arachidonic acid, namely ATL, by 12/15-lipoxygenase activity of acetylated COX2 (Clària and Serhan, 1995). This new class of endogenous autacoid functions as local anti-inflammatories displaying protective activities in peritonitis, dermal inflammation, reperfusion injury, asthma, angiogenesis, and periodontal disease (Chiang et al., 2005). As high doses and low doses of aspirin exert quite different roles, more attention must be paid to the doses when studying its actions.

Finally, BLT2 deficiency and the aspirin-dependent reduction in 12-HHT impaired re-epithelialization in vivo, whereas treatment with a BLT2 agonist improved re-epithelialization. Thus, our current data clarify the role of the 12-HHT/BLT2 axis in regulating keratinocyte migration by an increase in TNF and MMP9 levels during the re-epithelialization process, and also provide an answer to the question of how and by what mechanism high dose aspirin impedes skin repair. We anticipate that the current study results will evoke the caution of many clinicians regarding aspirin's inhibitory effect on wound healing, in addition to its notorious capacity to promote bleeding events.

MATERIALS AND METHODS

Mice and human samples. BLT1 KO (*Ltb4r1*$^{-/-}$), BLT2 KO (*Ltb4r2*$^{-/-}$), TxA_2S KO (*Tbxas1*$^{-/-}$), and TP KO (*Tbxa2r*$^{-/-}$) mice were generated as previously described (Kabashima et al., 2003; Terawaki et al., 2005; Iizuka et al., 2010; Matsunobu et al., 2013). Those mice are all backcrossed with C57BL/6J background strain for >12 generations. C57BL/6J and *db/db* mice were purchased from SLC Japan. In all experiments, 7–12-wk-old male mice were used. Except for TP KO mouse study, WT littermates have been used as control in all KO mouse experiments. All mice were maintained under a 12-h light/12-h dark cycle in a specific pathogen-free barrier facility. All studies and procedures were approved by the Ethics Committees on Animal Experimentation (Kyushu University) and Human Samples (Juntendo University).

Reagents. Aspirin, celecoxib, and actinomycin D were purchased from Sigma Aldrich. Heparin was obtained from Fuso Pharmaceutical Industries. Ozagrel, 12-HHT, LY255283, and CAY10583 were purchased from Cayman Chemical Company. Methyl cellulose 400 was purchased from Wako Pure Chemical Industries. Recombinant human TNF was obtained from PeproTech. The human TNF-neutralizing antibody Infliximab was purchased from Janssen Biotech. The mouse TNF-neutralizing antibody D2H4 was purchased from Cell Signaling Technology. MMP-9 inhibitor I (an MMP-9–specific reagent) and MMP inhibitor II (a broad MMP inhibitor) were purchased from EMD Millipore.

In vivo wound healing model. To obtain full-thickness skin excisions, 8-wk-old male mice were anesthetized, and six equidistant skin punches (3 mm in diameter) were made in the dorsal skin at six separate sites prepared with a depilatory agent. The wounds were allowed to heal uncovered, and the size of each wound was measured daily with a digital caliper. The wound areas were calculated, and the values were normalized to the initial area of the respective wound.

Quantification of 12-HHT in mouse serum, wound fluid, and skin. Blood was collected from the vena cava of 7-wk-old male C57BL/6J mice in a syringe with or without 1% (vol/vol) heparin and incubated at 37°C for 10 min. Treatment with aspirin (0.18 mg/ml in the drinking water) was initiated at 2 d before blood collection. In the ozagrel treatment group, mouse blood was collected by using a syringe containing ozagrel (10 μM final concentration).

Supernatants containing the serum fraction were prepared by centrifugation of the samples at 5,000 *g* for 10 min at 4°C.

To collect wound fluid, eight equidistant skin punches (3 mm in diameter) were made in the dorsal skin of 8-wk-old male C57BL/6J mice at eight separate sites prepared with a depilatory agent. The wounds were left undressed for the indicated time. Each wound was then washed with 60 µl phosphate buffered saline (−) magnesium and calcium (PBS (−)) containing 0.1% BSA (fatty acid free), and the wound wash fluids from the eight sites were pooled. 12-HHT was extracted and quantified as described previously (Kita et al., 2005; Matsunobu et al., 2013).

Histological analysis. Wounds with a 0.5-cm unwounded skin border were harvested and processed for histological analysis. The tissue samples were fixed in 10% formalin, paraffin-embedded, and stained with hematoxylin and eosin (HE). Wound lengths were measured as the distance between the wound margins. Re-epithelialization was defined as the migration distance of the neo-epidermis. The Ki67 antigen (a marker of proliferating cells) was visualized in paraffin-embedded 3-µm sections using a monoclonal antibody, NCL-Ki67-MM1 (Leica). Collagen deposition was evaluated in paraffin-embedded sections by Masson's trichrome staining. Histological analysis was performed by two board-certified dermatopathologists blinded to the experimental conditions.

Immunohistological staining. Paraffin sections of mouse skin were prepared at a thickness of 3 µm and baked overnight at 50°C. After deparaffinization and hydration, sections were pretreated for 5 min with 3% hydrogen peroxide (H_2O_2) and blocked for 20 min in PBS/5% goat serum (S1000; Vector Laboratories) at room temperature before staining with 0.25 µg/ml anti–mouse BLT2 polyclonal antibody (raised against mBLT2 C-tail in our laboratory) or 1 µg/ml of negative control rabbit IgG (DAKO) diluted with PBS/0.2% BSA overnight at 4°C. Sections were further stained with 3.3 µg/ml biotinylated goat anti–rabbit IgG secondary antibody (E432; DAKO) for 30 min at room temperature and then a streptavidin-HRP signal amplification step was performed using the TSA amplification kit (PerkinElmer) according to the instructions of the manufacturer. The horseradish peroxidase reaction was completed with 3, 3′-Diaminobenzidine (DAB; 0.009% in PBS; Dojindo Laboratories) and 0.004% hydrogen peroxide.

Paraffin sections of human skin were prepared at a thickness of 5 µm and baked overnight at 50°C. After deparaffinization and hydration, antigen retrieval was performed by heating in 10 mM citrate buffer, pH 6.0, for 5 min. Sections were permeabilized and blocked in PBS/0.1% Triton X-100/1% BSA for 10 min at room temperature before staining with 5 µg/ml anti–human BLT2 polyclonal antibody (Cayman) in PBS/0.1% Triton X-100/1% BSA overnight at 4°C. Sections were further stained with 10 µg/ml Alexa Fluor 488–conjugated goat anti–rabbit IgG secondary antibody (Life Technologies). Paraffin sections were mounted in ProLong Gold antifade reagent with DAPI (Invitrogen) and observed under a fluorescence microscope (BZ-9000; Keyence).

MPO assay. Skin samples were harvested by 5-mm punch biopsy as described above, weighed, homogenized in 50 mM potassium phosphate buffer, pH 6.5, containing 0.5% (wt/vol) hexadecyl trimethylammonium bromide at a 1:20 ratio (wt/vol), and then sonicated (2 × 30 s at 50 W). The sonicated samples were frozen, thawed, and subjected to centrifugation at 10,000 *g* for 10 min at 4°C. 10 µl of the supernatant was transferred to a 96-well plate containing 100 µl of reaction buffer (50 mM potassium phosphate buffer, pH 6.0, 0.157 mg/ml *o*-dianosidine [Sigma Aldrich], and 0.0005% hydrogen peroxide). Serial dilutions of commercially available MPO (EMD Millipore) were used as the standards. Absorbance at 450 nm was measured after incubation for 5 min.

Flow cytometry analysis of immune cells in the wounded skin. Wound tissue was collected from punch biopsy skin samples (5 mm in diameter), cut into small pieces, and incubated in a digestion buffer (PBS/10% FCS/1.2 mg/ml hyaluronidase [Sigma Aldrich]/1.6 mg/ml collagenase [Sigma Aldrich]/0.1 mg/ml DNase I [Sigma Aldrich]) at 37°C for 40 min. The digests were centrifuged at 1,500 rpm for 5 min and filtered through a nylon cell strainer (pore size, 40 µm). Cell pellets were resuspended in buffer (PBS/2% FCS/0.1% NaN_3), incubated with 5 µg/ml 2.4G2 antibody for 15 min to block Fcγ receptors, and stained with FITC-conjugated anti–Gr-1 (RB6-8C5), anti-CD4 (GK1.5), anti-B220 (RA3-6B2), allophycocyanin (APC)-conjugated anti-F4/80 (BM8), or phycoerythrin (PE)-conjugated anti-CD45.2 (104) antibody (eBioscience, all diluted 1:300) at 4°C for 30 min. Immune cells in the single-cell suspension were analyzed with a flow cytometer (BD).

MDA adduct ELISA. Skin samples were harvested by 5-mm punch biopsy as described above, weighed, and then homogenized in ice-cold PBS (−) at a 1:10 ratio (wt/vol). After centrifugation of the samples at 13,000 *g* for 10 min at 4°C, an MDA adduct ELISA was performed with the supernatants according to the manufacturer's protocol (OxiSelect MDA Adduct ELISA kit; Cell Biolabs).

Cell culture and transfection. Primary mouse keratinocytes and fibroblasts were isolated from neonatal mice. The keratinocytes were maintained in CnT-07 medium (CELLnTEC) according to a protocol modified from previously published procedures (Lichti et al., 2008). Primary mouse fibroblasts and immortalized human HaCaT keratinocytes were maintained in DMEM (Wako Pure Chemical Industries) containing 10% FCS (Gibco). Primary adult NHEKs and dermal fibroblasts were purchased from Lonza and maintained in keratinocyte or fibroblast growth medium supplemented with the compounds in the growth factor bullet kit (Lonza).

HaCaT cells were transfected with an expression vector for FLAG-tagged human BLT2 or the empty vector pCXN2 (Niwa et al., 1991). Stable transfectants were selected in the presence of 0.8 mg/ml G418 for 2 wk and then incubated with an anti-FLAG antibody (2H8; Sasaki et al., 2012), followed by an Alexa Fluor 488–conjugated goat anti–mouse IgG secondary antibody (Life Technologies). To avoid clonal variation, the BLT2-expressing cells were collected as polyclonal populations by cell sorting (FACSAria II; BD).

BrdU incorporation assay. The BrdU incorporation assay was performed using the colorimetric BrdU Cell Proliferation ELISA kit (Roche) according to the manufacturer's protocol. In brief, mouse primary keratinocytes were isolated from WT and BLT2 KO newborn mice and seeded onto collagen-I–coated 96-well plates at a density of 0.5×10^5 or 1.0×10^5 cells/well. The cells were cultured for 48 h, treated with 10 µM BrdU, and then cultured for an additional 12 h. BrdU incorporation was determined by measuring the absorbance at 450 nm.

In vitro scratch assay. Primary keratinocytes (3×10^5 cells/well), HaCaT cells (1.5×10^4 cells/well), and NHEKs (3.5×10^5 cells/well) were seeded onto a collagen-I–coated 96-well ImageLock tissue culture plate (Essen BioScience) and incubated in a standard CO_2 incubator for 48 h to form cell monolayers. Wounds were made with the 96-well WoundMaker (Essen BioScience). The wounded cells were washed twice with culture medium to remove the detached cells and then treated with 100 µl of medium containing appropriate concentrations of the test materials. Images of the wounds were automatically acquired within the CO_2 incubator by IncuCyte zoom software (Essen BioScience). Typical kinetic updates were taken at 3-h intervals for the duration of the experiment. The data were analyzed with respect to wound confluence and calculated by using the IncuCyte software package (Essen BioScience).

Quantification of cell death by propidium iodide (PI) staining. 12 h after scratching, 2.5 µg/ml PI (BD) was added to the HaCaT cells and after 10 min, the samples were analyzed by IN Cell Analyzer 1000 (GE Healthcare) according to the manufacturer's protocol. Cell death was quantified by calculating the percentage of PI-positive area to the whole cell area.

DNA microarray analysis. Total RNA was prepared from punch biopsies (5 mm in diameter) using the RNeasy Fibrous Tissue kit (QIAGEN). RNA from three mice per group was mixed and used for labeling. Probe cDNA was amplified and labeled with a total prep RNA amplification kit (Illumina)

according to the manufacturer's protocol and then used for hybridization with MouseWG-6 Expression BeadChip arrays (Illumina). The signals were quantified using the BeadStation with BeadArray technology, and the raw data were obtained using BeadStudio software (Illumina).

Q-PCR. Total RNA was prepared from cells using TRIzol reagent (Life Technologies), or from punch biopsies (5 mm diameter) using the RNeasy Fibrous Tissue kit (QIAGEN). 1 µg of total RNA was used for the RT reaction (QuantiTect Reverse Transcription kit; QIAGEN). Target genes were detected by real-time PCR with Takara SYBR Premix Ex Taq II (Takara Bio Inc.). The sequences of the primers were as follows: mouse BLT2 (*Ltb4r2*) upstream region, 5′-ACAGCCTTGGCTTTCTTCAG-3′, and downstream, 5′-TGCCCCATTACTTTCAGCTT-3′; mouse TNF (*Tnf*) upstream, 5′-GGTGCCTATGTCTCAGCCTCTT-3′, and downstream, 5′-CGATCACCCCGAAGTTCAGTA-3′; mouse IL-1β (*Il1b*) upstream, 5′-TCCAGGATGAGGACATGAGCAC-3′, and downstream, 5′-GAACGTCACACACCAGCAGGTTA-3′; mouse MMP9 (*Mmp9*) upstream, 5′-GCCCTGGAACTCACACGACA-3′, and downstream, 5′-TTGGAAACTCACACGCCAGAAG-3′; human TNF (*TNF*) upstream, 5′-CTGCTGCACTTTGGAGTGAT-3′, and downstream, 5′-AGATGATCTGACTGCCTGGG-3′; human IL-1β (*IL1B*) upstream, 5′-GCCCTAAACAGATGAAGTGCTC-3′, and downstream, 5′-GAACCAGCATCTTCCTCAG-3′; human MMP9 (*MMP9*) upstream, 5′-GACGCAGACATCGTCATCCAGTTT-3′, and downstream, 5′-GCCGCGCCATCTGCGTTT-3′; human β-actin (*ACTB*) upstream, 5′-TGGCACCCAGCACAATGAA-3′, and downstream, 5′-CTAAGTCATAGTCCGCCTAGAAGCA-3′; and mouse β-actin (*Actb*) upstream, 5′-CATCCGTAAAGACCTCTATGCCAAC-3′, and downstream, 5′-ATGGAGCCACCGATCCACA-3′; mouse r18S (*Rps18*) upstream, 5′-TTCTGGCCAACGGTCTAGACAAC-3′, and downstream, 5′-CCAGTGGTCTTGGTGTGCTGA-3′. For the detection of human BLT2 (*LTB4R2*), real-time PCR was performed by using the LightCycler TaqMan Master kit with Universal Probe Library Probe #74 (Roche) and the primers 5′-GGCCTTGGCCTTCTTCAG-3′ (left) and 5′-GTGAGGAAACGGGGACCT-3′ (right). PCR was monitored via the LightCycler System (Roche). Gene expression levels were determined with the ΔΔCT method after normalization to the expression level of the standard housekeeping gene β-actin in all experiments, except for the mouse skin Q-PCR in which r18S was used.

Cytometric bead array (CBA). HaCaT-mock and HaCaT-BLT2 cells were seeded onto 24-well plates at a density of 7.5×10^4 cells/well in 500 µl DMEM containing 10% FCS. After 36 h, the cells were stimulated with 1 µM 12-HHT for another 6 h. CBA analysis was performed with 50 µl of supernatant and the BD CBA Human TNF Enhanced Sensitivity Flex Set (BD) according to the manufacturer's protocol.

Gelatin zymography. HaCaT-mock and HaCaT-BLT2 cells were seeded onto 12-well plates at a density of 1.5×10^5 cells/well in 500 µl DMEM containing 10% FCS. After 24 h, the cells were serum-starved for 3 h and then stimulated with test materials for another 24 h. The supernatants were concentrated fivefold using an Amicon Ultra-0.5 Centrifugal Filter with a molecular weight cutoff (MWCO) of 30 K (Millipore). A 20-µl aliquot of the concentrated supernatant was separated on a 10% acrylamide gelatin gel (1 mg/ml gelatin, 10% acrylamide-bisacrylamide, 375 mM Tris, pH 8.8, 0.4% glycerol, 0.08% sodium dodecyl sulfate [SDS], 0.05% TEMED, and 0.5% ammonium persulfate) alongside human MMP9 reference standards (R&D Systems). The gel was washed in 2.5% Triton X-100, incubated overnight at 37°C in a renaturing buffer (50 mM Tris, pH 7.4, 5 mM $CaCl_2$, 1 µM $ZnCl_2$, and 0.01% sodium azide), stained with 0.1% Coomassie R250 in 50% methanol/10% acetic acid for 30 min, and destained in 10% methanol/7% acetic acid.

Dual luciferase assay. Double-strand DNA containing 5×NF-κB RE (5× 5′-GGGGACTTTCC-3′) or 5×mutated NF-κB RE (5× 5′-GGTTACTTTAA-3′) was inserted into NheI–HindIII site of pGL4.23 (Promega). HaCaT-mock and HaCaT-BLT2 cells were seeded onto 12-well plates at a density of 1.75×10^5 cells/well in DMEM containing 10% FCS and cultured for 24 h. The cells were washed twice with FCS-free DMEM, followed by the addition of 1 ml DMEM containing 10% charcoal-treated FCS. After 2 h, the cells were co-transfected with pGL4.23-5×NF-κB RE or pGL4.23-5×mutated NF-κB RE and pGL4.74 [*hRluc*/TK] (Promega) using Lipofectamine LTX (Life Technologies). 18 h later, the cells were stimulated with 1 µM 12-HHT for another 6 h. Lysates were prepared by adding 200 µl lysis buffer (Tokyo Ink), and firefly and Renilla (sea pansy) luciferase activities were measured with the PicaGene Dual Sea Pansy Luminescence kit (Tokyo Ink).

Mouse MMP9 ELISA. Mouse primary keratinocyte were isolated from BLT2 WT and BLT2 KO littermates and seeded onto 12-well plates at a density of 0.8×10^6 cells/well in CnT-07 medium (CELLnTEC). After 12 and 24 h, the supernatants were collected and concentrated fivefold using an Ultra-0.5 Centrifugal Filter (Amicon) with a molecular weight cutoff (MWCO) of 30 K (Millipore). ELISA analysis was performed with 50 µl of concentrated supernatant and the Mouse Total MMP-9 Quantikine ELISA kit (R&D Systems) according to the manufacturer's protocol.

Statistical analysis. Data are presented as the mean ± SEM. All statistical analyses were performed using unpaired Student's *t* test (two groups) or ANOVA (greater than two groups), with post hoc tests to compare with each group. All statistics were calculated by Prism 5 software (GraphPad Software).

Online supplemental material. The time-lapse movies in Video 1, covering a period of 72 h, show the migration of BLT2 WT mouse primary keratinocytes. The time-lapse movies in Video 2, covering a period of 72 h, show the migration of BLT2 KO mouse primary keratinocytes. The time-lapse movies in Video 3, covering a period of 48 h, show the migration of HaCaT-mock cells cultured in medium containing 0.5% FCS. The time-lapse movies in Video 4, covering a period of 48 h, show the migration of HaCaT-BLT2 cells cultured in medium containing 0.5% FCS. Online supplemental material is available at http://www.jem.org/cgi/content/full/jem.20132063/DC1.

We thank the Support Center for Education and Research (Kyushu University) for technical support and Junichi Miyazaki (Osaka University) for supplying the pCXN2 expression vector. We also thank Hiromi Doi (Kyoto University), Yuka Eguchi (Kyushu University), and Atsushi Furuhata (Juntendo University) for technical support and Masutaka Furue (Kyushu University), Soh Yamazaki (Kyushu University), Makoto Arita (The University of Tokyo), and the members of our laboratories for advice and helpful discussions.

M. Liu is a Research Fellow of the Japan Society for the Promotion of Science. This work was supported by Grants-in-Aid for Scientific Research from the Ministry of Education, Culture, Sports, Science, and Technology of Japan (Nos. 21390083, 22116001, and 22116002 to T. Yokomizo; Nos. 22790320 and 24590386 to K. Saeki; and Nos. 24102522 and 25460374 to T. Okuno), the Naito Foundation, Ono Medical Research Foundation, the Uehara Memorial Foundation, the Fukuoka Foundation for Sound Health, the Takeda Science Foundation, and the Inamori Foundation.

The authors declare no competing financial interests.

Submitted: 29 September 2013
Accepted: 7 April 2014

REFERENCES

Arita, M., M. Yoshida, S. Hong, E. Tjonahen, J.N. Glickman, N.A. Petasis, R.S. Blumberg, and C.N. Serhan. 2005. Resolvin E1, an endogenous lipid mediator derived from omega-3 eicosapentaenoic acid, protects against 2,4,6-trinitrobenzene sulfonic acid-induced colitis. *Proc. Natl. Acad. Sci. USA*. 102:7671–7676. http://dx.doi.org/10.1073/pnas.0409271102

Awtry, E.H., and J. Loscalzo. 2000. Aspirin. *Circulation*. 101:1206–1218. http://dx.doi.org/10.1161/01.CIR.101.10.1206

Baum, C.L., and C.J. Arpey. 2005. Normal cutaneous wound healing: clinical correlation with cellular and molecular events. *Dermatol. Surg.* 31:674–686.

Borzini, P., and L. Mazzucco. 2005. Platelet gels and releasates. *Curr. Opin. Hematol.* 12:473–479. http://dx.doi.org/10.1097/01.moh.0000177831.70657.e8

Brem, H., and M. Tomic-Canic. 2007. Cellular and molecular basis of wound healing in diabetes. *J. Clin. Invest.* 117:1219–1222. http://dx.doi.org/10.1172/JCI32169

Chan, A.T., S. Ogino, and C.S. Fuchs. 2007. Aspirin and the risk of colorectal cancer in relation to the expression of COX-2. *N. Engl. J. Med.* 356:2131–2142. http://dx.doi.org/10.1056/NEJMoa067208

Chiang, N., M. Arita, and C.N. Serhan. 2005. Anti-inflammatory circuitry: lipoxin, aspirin-triggered lipoxins and their receptor ALX. *Prostaglandins Leukot. Essent. Fatty Acids.* 73:163–177. http://dx.doi.org/10.1016/j.plefa.2005.05.003

Cho, K.J., J.M. Seo, Y. Shin, M.H. Yoo, C.S. Park, S.H. Lee, Y.S. Chang, S.H. Cho, and J.H. Kim. 2010. Blockade of airway inflammation and hyperresponsiveness by inhibition of BLT2, a low-affinity leukotriene B4 receptor. *Am. J. Respir. Cell Mol. Biol.* 42:294–303. http://dx.doi.org/10.1165/rcmb.2008-0445OC

Clària, J., and C.N. Serhan. 1995. Aspirin triggers previously undescribed bioactive eicosanoids by human endothelial cell-leukocyte interactions. *Proc. Natl. Acad. Sci. USA.* 92:9475–9479. http://dx.doi.org/10.1073/pnas.92.21.9475

Cogswell, J.P., M.M. Godlevski, G.B. Wisely, W.C. Clay, L.M. Leesnitzer, J.P. Ways, and J.G. Gray. 1994. NF-kappa B regulates IL-1 beta transcription through a consensus NF-kappa B binding site and a nonconsensus CRE-like site. *J. Immunol.* 153:712–723.

Coulombe, P.A. 2003. Wound epithelialization: accelerating the pace of discovery. *J. Invest. Dermatol.* 121:219–230. http://dx.doi.org/10.1046/j.1523-1747.2003.12387.x

Demidova-Rice, T.N., L. Wolf, J. Deckenback, M.R. Hamblin, and I.M. Herman. 2012. Human platelet-rich plasma- and extracellular matrix-derived peptides promote impaired cutaneous wound healing in vivo. *PLoS ONE.* 7:e32146. http://dx.doi.org/10.1371/journal.pone.0032146

Esterbauer, H., R.J. Schaur, and H. Zollner. 1991. Chemistry and biochemistry of 4-hydroxynonenal, malonaldehyde and related aldehydes. *Free Radic. Biol. Med.* 11:81–128. http://dx.doi.org/10.1016/0891-5849(91)90192-6

Falanga, V., F. Grinnell, B. Gilchrest, Y.T. Maddox, and A. Moshell. 1994. Workshop on the pathogenesis of chronic wounds. *J. Invest. Dermatol.* 102:125–127. http://dx.doi.org/10.1111/1523-1747.ep12371745

Fang, R.C., and R.D. Galiano. 2008. A review of becaplermin gel in the treatment of diabetic neuropathic foot ulcers. *Biologics.* 2:1–12.

Fu, X., X. Li, B. Cheng, W. Chen, and Z. Sheng. 2005. Engineered growth factors and cutaneous wound healing: success and possible questions in the past 10 years. *Wound Repair Regen.* 13:122–130. http://dx.doi.org/10.1111/j.1067-1927.2005.130202.x

Gillitzer, R., and M. Goebeler. 2001. Chemokines in cutaneous wound healing. *J. Leukoc. Biol.* 69:513–521.

Greenhalgh, D.G., K.H. Sprugel, M.J. Murray, and R. Ross. 1990. PDGF and FGF stimulate wound healing in the genetically diabetic mouse. *Am. J. Pathol.* 136:1235–1246.

Group, S.C. 1989. Final Report on the Aspirin Component of the Ongoing Physicians' Health Study. *N. Engl. J. Med.* 321:129–135. http://dx.doi.org/10.1056/NEJM198907203210301

Hamberg, M., J. Svensson, and B. Samuelsson. 1974. Prostaglandin endoperoxides. A new concept concerning the mode of action and release of prostaglandins. *Proc. Natl. Acad. Sci. USA.* 71:3824–3828. http://dx.doi.org/10.1073/pnas.71.10.3824

Hennig, R., T. Osman, I. Esposito, N. Giese, S.M. Rao, X.Z. Ding, W.G. Tong, M.W. Büchler, T. Yokomizo, H. Friess, and T.E. Adrian. 2008. BLT2 is expressed in PanINs, IPMNs, pancreatic cancer and stimulates tumour cell proliferation. *Br. J. Cancer.* 99:1064–1073. http://dx.doi.org/10.1038/sj.bjc.6604655

Holvoet, S., C. Vincent, D. Schmitt, and M. Serres. 2003. The inhibition of MAPK pathway is correlated with down-regulation of MMP-9 secretion induced by TNF-α in human keratinocytes. *Exp. Cell Res.* 290:108–119. http://dx.doi.org/10.1016/S0014-4827(03)00293-3

Iizuka, Y., T. Yokomizo, K. Terawaki, M. Komine, K. Tamaki, and T. Shimizu. 2005. Characterization of a mouse second leukotriene B4 receptor, mBLT2: BLT2-dependent ERK activation and cell migration of primary mouse keratinocytes. *J. Biol. Chem.* 280:24816–24823. http://dx.doi.org/10.1074/jbc.M413257200

Iizuka, Y., T. Okuno, K. Saeki, H. Uozaki, S. Okada, T. Misaka, T. Sato, H. Toh, M. Fukayama, N. Takeda, et al. 2010. Protective role of the leukotriene B4 receptor BLT2 in murine inflammatory colitis. *FASEB J.* 24:4678–4690. http://dx.doi.org/10.1096/fj.10-165050

Jeffcoate, W.J., and K.G. Harding. 2003. Diabetic foot ulcers. *Lancet.* 361:1545–1551. http://dx.doi.org/10.1016/S0140-6736(03)13169-8

Kabashima, K., T. Murata, H. Tanaka, T. Matsuoka, D. Sakata, N. Yoshida, K. Katagiri, T. Kinashi, T. Tanaka, M. Miyasaka, et al. 2003. Thromboxane A2 modulates interaction of dendritic cells and T cells and regulates acquired immunity. *Nat. Immunol.* 4:694–701. http://dx.doi.org/10.1038/ni943

Kamohara, M., J. Takasaki, M. Matsumoto, T. Saito, T. Ohishi, H. Ishii, and K. Furuichi. 2000. Molecular cloning and characterization of another leukotriene B4 receptor. *J. Biol. Chem.* 275:27000–27004.

Kaushal, M., N. Gopalan Kutty, and C. Mallikarjuna Rao. 2007. Wound healing activity of NOE-aspirin: a pre-clinical study. *Nitric Oxide.* 16:150–156. http://dx.doi.org/10.1016/j.niox.2006.07.004

Kendall, A.C., and A. Nicolaou. 2013. Bioactive lipid mediators in skin inflammation and immunity. *Prog. Lipid Res.* 52:141–164. http://dx.doi.org/10.1016/j.plipres.2012.10.003

Kita, Y., T. Takahashi, N. Uozumi, and T. Shimizu. 2005. A multiplex quantitation method for eicosanoids and platelet-activating factor using column-switching reversed-phase liquid chromatography-tandem mass spectrometry. *Anal. Biochem.* 342:134–143. http://dx.doi.org/10.1016/j.ab.2005.03.048

Kuprash, D.V., I.A. Udalova, R.L. Turetskaya, D. Kwiatkowski, N.R. Rice, and S.A. Nedospasov. 1999. Similarities and differences between human and murine TNF promoters in their response to lipopolysaccharide. *J. Immunol.* 162:4045–4052.

Kyriakides, T.R., D. Wulsin, E.A. Skokos, P. Fleckman, A. Pirrone, J.M. Shipley, R.M. Senior, and P. Bornstein. 2009. Mice that lack matrix metalloproteinase-9 display delayed wound healing associated with delayed reepithelization and disordered collagen fibrillogenesis. *Matrix Biol.* 28:65–73. http://dx.doi.org/10.1016/j.matbio.2009.01.001

Lichti, U., J. Anders, and S.H. Yuspa. 2008. Isolation and short-term culture of primary keratinocytes, hair follicle populations and dermal cells from newborn mice and keratinocytes from adult mice for in vitro analysis and for grafting to immunodeficient mice. *Nat. Protoc.* 3:799–810. http://dx.doi.org/10.1038/nprot.2008.50

Luster, A.D., and A.M. Tager. 2004. T-cell trafficking in asthma: lipid mediators grease the way. *Nat. Rev. Immunol.* 4:711–724. http://dx.doi.org/10.1038/nri1438

Martin, P. 1997. Wound healing—aiming for perfect skin regeneration. *Science.* 276:75–81. http://dx.doi.org/10.1126/science.276.5309.75

Mathis, S., V.R. Jala, and B. Haribabu. 2007. Role of leukotriene B4 receptors in rheumatoid arthritis. *Autoimmun. Rev.* 7:12–17. http://dx.doi.org/10.1016/j.autrev.2007.03.005

Matsunobu, T., T. Okuno, C. Yokoyama, and T. Yokomizo. 2013. Thromboxane A synthase-independent production of 12-hydroxyheptadecatrienoic acid, a BLT2 ligand. *J. Lipid Res.* 54:2979–2987. http://dx.doi.org/10.1194/jlr.M037754

Mayser, P., H. Grimm, and F. Grimminger. 2002. n-3 fatty acids in psoriasis. *Br. J. Nutr.* 87:S77–S82. http://dx.doi.org/10.1079/BJN2001459

McGrath, J.A., and S.M. Breathnach. 2004. Wound healing. *In* Rook's Textbook of Dermatology. T. Burns, S. Breathnach, N. Cox, and C. Griffiths, editors. Blackwell Science, Oxford. 11.11–11.25.

Miki, Y., K. Yamamoto, Y. Taketomi, H. Sato, K. Shimo, T. Kobayashi, Y. Ishikawa, T. Ishii, H. Nakanishi, K. Ikeda, et al. 2013. Lymphoid tissue phospholipase A2 group IID resolves contact hypersensitivity by driving antiinflammatory lipid mediators. *J. Exp. Med.* 210:1217–1234. http://dx.doi.org/10.1084/jem.20121887

Morris, T., M. Stables, A. Hobbs, P. de Souza, P. Colville-Nash, T. Warner, J. Newson, G. Bellingan, and D.W. Gilroy. 2009. Effects of low-dose aspirin on acute inflammatory responses in humans. *J. Immunol.* 183:2089–2096. http://dx.doi.org/10.4049/jimmunol.0900477

Niwa, H., K. Yamamura, and J. Miyazaki. 1991. Efficient selection for high-expression transfectants with a novel eukaryotic vector. *Gene.* 108:193–199. http://dx.doi.org/10.1016/0378-1119(91)90434-D

Norling, L.V., M. Spite, R. Yang, R.J. Flower, M. Perretti, and C.N. Serhan. 2011. Cutting edge: Humanized nano-proresolving medicines mimic inflammation-resolution and enhance wound healing. *J. Immunol.* 186:5543–5547. http://dx.doi.org/10.4049/jimmunol.1003865

Okuno, T., Y. Iizuka, H. Okazaki, T. Yokomizo, R. Taguchi, and T. Shimizu. 2008. 12(S)-Hydroxyheptadeca-5Z, 8E, 10E-trienoic acid is a natural ligand for leukotriene B4 receptor 2. *J. Exp. Med.* 205:759–766. http://dx.doi.org/10.1084/jem.20072329

Pollack, S.V. 1984. Systemic drugs and nutritional aspects of wound healing. *Clin. Dermatol.* 2:68–80. http://dx.doi.org/10.1016/0738-081X(84)90028-2

Sasaki, F., T. Okuno, K. Saeki, L. Min, N. Onohara, H. Kato, T. Shimizu, and T. Yokomizo. 2012. A high-affinity monoclonal antibody against the FLAG tag useful for G-protein-coupled receptor study. *Anal. Biochem.* 425:157–165. http://dx.doi.org/10.1016/j.ab.2012.03.014

Scott, K.A., C.H. Arnott, S.C. Robinson, R.J. Moore, R.G. Thompson, J.F. Marshall, and F.R. Balkwill. 2004. TNF-alpha regulates epithelial expression of MMP-9 and integrin αvβ6 during tumour promotion. A role for TNF-α in keratinocyte migration? *Oncogene.* 23:6954–6966. http://dx.doi.org/10.1038/sj.onc.1207915

Serhan, C.N., S. Yacoubian, and R. Yang. 2008. Anti-inflammatory and proresolving lipid mediators. *Annu. Rev. Pathol.* 3:279–312. http://dx.doi.org/10.1146/annurev.pathmechdis.3.121806.151409

Seta, F., A.D. Chung, P.V. Turner, J.D. Mewburn, Y. Yu, and C.D. Funk. 2009. Renal and cardiovascular characterization of COX-2 knockdown mice. *Am. J. Physiol. Regul. Integr. Comp. Physiol.* 296:R1751–R1760. http://dx.doi.org/10.1152/ajpregu.90985.2008

Shao, W.H., A. Del Prete, C.B. Bock, and B. Haribabu. 2006. Targeted disruption of leukotriene B4 receptors BLT1 and BLT2: a critical role for BLT1 in collagen-induced arthritis in mice. *J. Immunol.* 176:6254–6261. http://dx.doi.org/10.4049/jimmunol.176.10.6254

Singer, A.J., and R.A. Clark. 1999. Cutaneous wound healing. *N. Engl. J. Med.* 341:738–746. http://dx.doi.org/10.1056/NEJM199909023411006

Stojadinovic, O., H. Brem, C. Vouthounis, B. Lee, J. Fallon, M. Stallcup, A. Merchant, R.D. Galiano, and M. Tomic-Canic. 2005. Molecular pathogenesis of chronic wounds: the role of β-catenin and *c-myc* in the inhibition of epithelialization and wound healing. *Am. J. Pathol.* 167:59–69. http://dx.doi.org/10.1016/S0002-9440(10)62953-7

Sugimoto, Y., A. Yamasaki, E. Segi, K. Tsuboi, Y. Aze, T. Nishimura, H. Oida, N. Yoshida, T. Tanaka, M. Katsuyama, et al. 1997. Failure of parturition in mice lacking the prostaglandin F receptor. *Science.* 277:681–683. http://dx.doi.org/10.1126/science.277.5326.681

Terawaki, K., T. Yokomizo, T. Nagase, A. Toda, M. Taniguchi, K. Hashizume, T. Yagi, and T. Shimizu. 2005. Absence of leukotriene B4 receptor 1 confers resistance to airway hyperresponsiveness and Th2-type immune responses. *J. Immunol.* 175:4217–4225. http://dx.doi.org/10.4049/jimmunol.175.7.4217

Werner, S., and R. Grose. 2003. Regulation of wound healing by growth factors and cytokines. *Physiol. Rev.* 83:835–870.

Woodward, D.F., R.L. Jones, and S. Narumiya. 2011. International Union of Basic and Clinical Pharmacology. LXXXIII: classification of prostanoid receptors, updating 15 years of progress. *Pharmacol. Rev.* 63:471–538. http://dx.doi.org/10.1124/pr.110.003517

Yokomizo, T., T. Izumi, K. Chang, Y. Takuwa, and T. Shimizu. 1997. A G-protein-coupled receptor for leukotriene B4 that mediates chemotaxis. *Nature.* 387:620–624. http://dx.doi.org/10.1038/42506

Yokomizo, T., K. Kato, K. Terawaki, T. Izumi, and T. Shimizu. 2000a. A second leukotriene B(4) receptor, BLT2. A new therapeutic target in inflammation and immunological disorders. *J. Exp. Med.* 192:421–432. http://dx.doi.org/10.1084/jem.192.3.421

Yokomizo, T., K. Masuda, K. Kato, A. Toda, T. Izumi, and T. Shimizu. 2000b. Leukotriene B_4 receptor. Cloning and intracellular signaling. *Am. J. Respir. Crit. Care Med.* 161:S51–S55. http://dx.doi.org/10.1164/ajrccm.161.supplement_1.ltta-11

Yokomizo, T., K. Kato, H. Hagiya, T. Izumi, and T. Shimizu. 2001. Hydroxyeicosanoids bind to and activate the low affinity leukotriene B4 receptor, BLT2. *J. Biol. Chem.* 276:12454–12459. http://dx.doi.org/10.1074/jbc.M011361200

Yoo, M.H., H. Song, C.H. Woo, H. Kim, and J.H. Kim. 2004. Role of the BLT2, a leukotriene B4 receptor, in Ras transformation. *Oncogene.* 23:9259–9268.

Yu, Z., C. Schneider, W.E. Boeglin, and A.R. Brash. 2005. Mutations associated with a congenital form of ichthyosis (NCIE) inactivate the epidermal lipoxygenases 12R-LOX and eLOX3. *Biochim. Biophys. Acta.* 1686:238–247. http://dx.doi.org/10.1016/j.bbalip.2004.10.007

Ziboh, V.A., C.C. Miller, and Y. Cho. 2000. Significance of lipoxygenase-derived monohydroxy fatty acids in cutaneous biology. *Prostaglandins Other Lipid Mediat.* 63:3–13. http://dx.doi.org/10.1016/S0090-6980(00)00093-9